Archives of Virology (2023) 168:147
https://doi.org/10.1007/s00705-023-05770-1

ORIGINAL ARTICLE

Repurposing of artesunate, an antimalarial drug, as a potential inhibitor of hepatitis E virus

Neha Bhise[1] · Megha Agarwal[2] · Nidhi Thakur[1] · P. S. Akshay[1] · Sarah Cherian[4] · Kavita Lole[3]

Received: 16 July 2022 / Accepted: 29 March 2023 / Published online: 28 April 2023

Abstract

Hepatitis E virus (HEV) is endemic in several developing countries of Africa and Asia. It mainly causes self-limiting waterborne infections, in either sporadic or outbreak form. Recently, HEV was shown to cause chronic infections in immunosuppressed individuals. Ribavirin and interferon, the current off-label treatment options for hepatitis E, have several side effects. Hence, there is a need for new drugs. We evaluated the antimalarial drug artesunate (ART) against genotype 1 HEV (HEV-1) and HEV-3 using a virus-replicon-based cell culture system. ART exhibited 59% and 43% inhibition of HEV-1 and HEV-3, respectively, at the highest nontoxic concentration. Computational molecular docking analysis showed that ART can bind to the helicase active site (affinity score, -7.4 kcal/mol), indicating its potential to affect ATP hydrolysis activity. An *in vitro* ATPase activity assay of the helicase indeed showed 24% and 55% inhibition at 19.5 µM (EC_{50}) and 78 µM concentrations of ART, respectively. Since ATP is a substrate of RNA-dependent RNA polymerase (RdRp) as well, we evaluated the effect of ART on the enzymatic activity of the viral polymerase. Interestingly, ART showed 26% and 40% inhibition of the RdRp polymerase activity at 19.5 µM and 78 µM concentrations of ART, respectively. It could be concluded from these findings that ART inhibited replication of both HEV-1 and HEV-3 by directly targeting the activities of the viral enzymes helicase and RdRp. Considering that ART is known to be safe in pregnant women, we think this antimalarial drug deserves further evaluation in animal models.

Abbreviations

HEV	Hepatitis E virus
HEV-1 & 3	HEV genotypes 1 and 3
ART	Artesunate
SG	Subgenome
FG	Full genome
CQ	Chloroquine
HCQ	Hydroxychloroquine
RBV	Ribavirin
RTP	Ribavirin triphosphate
HCV	Hepatitis C virus

Handling Editor: Michael A. Purdy.

✉ Sarah Cherian
sarahcherian100@gmail.com

✉ Kavita Lole
lolekavita37@yahoo.com

[1] Hepatitis Group, Indian Council of Medical Research-National Institute of Virology, Microbial Containment Complex, Pune, India

[2] Bioinformatics and Data Management Group, Indian Council of Medical Research-National Institute of Virology, Dr. Ambedkar Road, Pune, India

[3] Hepatitis Group, ICMR-National Institute of Virology, Microbial Containment Complex, Sus Road, Pashan, Pune 411021, India

[4] Bioinformatics and Data Management Group, ICMR-National Institute of Virology, 20-A, Dr. Ambedkar Road, Pune 411001, India

Introduction

Hepatitis E virus (HEV) is the global cause of acute viral hepatitis, with ~3.3 million cases and 44,000-70,000 deaths annually (~3.3% of the total mortality due to viral hepatitis) [1]. HEV exhibits the highest seroprevalence in developing countries due to poor drinking water quality and improper sanitation conditions [2–4]. HEV-1 and HEV-2 infect only humans and mainly cause self-limiting waterborne infections in developing countries [5, 6]. Hepatitis E can lead to adverse outcomes in old age and in patients with preexisting liver disease [7, 8]. HEV infection during the third trimester of pregnancy accounts for ~20-25% of maternal deaths and stillbirths [9, 10]. Although hepatitis E was previously thought to be a problem only in developing countries,

in the last two decades, autochthonous HEV-3 and HEV-4 infections have been reported in industrialized countries [11, 12]. HEV-3 and HEV-4 are animal viruses that occasionally infect humans and cause infections that are usually self-limiting [13]. Although HEV-3 is not known to cause severe infections in pregnant women, it can cause chronic infections in immunocompromised individuals that may lead to the rapid progression of cirrhosis [14]. A recent study in Switzerland showed that males of older age are at high risk of HEV-3 and HEV-4 infections [15]. Chronicity due to HEV-1 has been reported in developing regions, but it is comparatively rare [16, 17].

HEV belongs to the family *Hepeviridae*, which is divided into two subfamilies: *Orthohepevirinae* and *Parahepevirinae* [18, 19]. The subfamily *Orthohepevirinae* includes viral variants that infect humans. HEV is a quasi-enveloped, single-strand, positive-sense RNA virus with a ~7.2-kb genome [20]. The viral genome has a 5' methylguanosine cap, a 5' non-coding region followed by three open reading frames (ORFs) – ORF1, ORF2, and ORF3 – and a 3' non-coding region with a polyadenylated tail. ORF1 encodes nonstructural protein domains, including methyltransferase [MeT], Y domain, papain-like cysteine protease [PCP], macrodomain [X], RNA helicase [Hel], and RNA-dependent RNA polymerase [RdRp]. ORF2 encodes the viral capsid/ORF2 protein, and ORF3 encodes a functional ion channel protein that plays a crucial role in the release of virus particles [21–23]. HEV-1 has an additional ORF, ORF4, encoding a protein that is believed to help the functioning of the viral polymerase [24].

HEV is transmitted via the feco-oral route through contaminated water and food. Water-borne transmission is the most common route for HEV-1 and HEV-2 transmission in resource-limited settings, while food-borne transmission is the predominant mode in endemic developed countries that experience sporadic cases [25]. HEV-3 and 4 are associated with food-borne zoonotic transmission due to the consumption of meat or meat products prepared from infected animals [26]. Pigs have been shown to be the principal source of zoonotic transmission of the virus. HEV contamination has been detected in dry-cured pork products and pork liver sausages (consisting of raw liver) in European countries with heavy pork diets. Contamination of water bodies with ground water or sewage from pig farms has also been shown to spread HEV-3 and HEV-4 [27, 28].

Immunosuppressive therapies have been used for treating chronic hepatitis E [29, 30]. Moreover, although there is some off-label use of ribavirin (RBV) and pegylated interferon-α [PEG-IFNα] therapy, this is associated with severe side effects and the emergence of viral resistance, making it a less-than-ideal treatment option [31–34]. Ribavirin is contraindicated during pregnancy due to its teratogenic effects [35]. Due to the drawbacks of ribavirin, direct-acting antiviral such as sofosbuvir came to light and was found to be effective against HEV-1 and HEV-3 [36]. Hence, there is a need for new antivirals that are safe for pregnant women and effective in chronic hepatitis E cases.

Drug repurposing is an attractive strategy that uses a combination of experimental and *in silico*-based approaches to identify novel pharmacological applications of available drugs [37]. A recent study by Galani et al. [38] showed that antimalarial drugs such as amodiaquine and lumefantrine are good candidates for use against HEV. The authors used both *in silico* and *in vitro* approaches to screen eight licensed antimalarial drugs against HEV. Artemisinin, a natural product obtained from the Chinese herb *Artemisia annua* [39], was also included in the study; however, it was not studied further because it showed a low binding affinity for HEV proteins. WHO has endorsed the use of artemisinin and its derivatives, such as artesunate [ART] and artemether, for the treatment of severe malaria during pregnancy [40]. ART is a hemisuccinate derivative of dihydroartemisinin and a highly potent compound with enhanced water solubility [41]. Artemisinin and ART have anticancer [42], anti-schistosomiasis [43], and antiviral activity [44–46]. Antiviral activity of ART has been shown against HIV-1 [47] and hepatitis B and C viruses [48–50]. In the present study, evaluation of ART against HEV using a replicon-base screening system showed >50% inhibition of replication of an HEV subgenomic replicon, suggesting a possible influence on HEV nonstructural proteins such as the RdRp, helicase, protease, etc. To understand the mode of action of ART, we carried out a molecular docking simulation of ART on HEV helicase. Interestingly, ART showed binding at the NTP-binding site of HEV helicase with high affinity. Furthermore, *in vitro* enzymatic assays carried out in the presence of ART showed inhibition of the ATPase activity of HEV helicase. Although Galani *et al.* reported a low affinity of artemisinin for HEV RdRp, our *in vitro* RdRp polymerase assays showed that ART (an artemisinin derivative) also inhibited enzymatic activity, suggesting that ART is a direct-acting non-nucleotide drug that inhibits virus replication by targeting the helicase and polymerase activities of HEV by blocking the ATP-binding sites of these enzymes.

Materials and methods

Cells, clones, and expression plasmids

Huh-7-derived clonal S10-3 cells, pSK-HEV-2 (an HEV-1 full-genome infectious cDNA clone [GenBank accession no. AF444002]) [51], and pSK P6-RLuc (an HEV-3 subgenomic clone [GenBank accession no. JQ679013]) [52] were a kind gift from Dr. S. Emerson, National Institutes of Health, Bethesda, MD, USA. The HEV-1 subgenomic replicon clone

pSK-HEV-Rluc containing a *Renilla* luciferase (Rluc) gene was a kind gift from Dr. X. J. Meng (Virginia Tech, Blacksburg, VA, USA) [53].

Drugs

The approved antimalarial drugs chloroquine (CQ; Abcam, cat. no. ab142116), hydroxychloroquine (HCQ; Abcam, cat. no. ab120827), artesunate (ART; Sigma-Aldrich, cat. no. A3731), and ribavirin (RBV; Santa Cruz Biotechnology, cat. no. sc-358731), which was used as a positive control, were tested for their inhibitory activity against HEV. Ribavirin triphosphate (RTP; Santa Cruz Biotechnology, cat. no. sc-358826) was used as a positive control for *in vitro* enzymatic assays. Stock solutions were prepared in nuclease-free water for chloroquine (1 mM), hydroxychloroquine (1 mM), ribavirin (2 mM), and ribavirin triphosphate (1 mM) and in 100% acetone for artesunate (86 mM). A working solution of 1 mM artesunate was prepared in nuclease-free water. Stock solutions of all drugs were stored at -20° C in aliquots until use.

Cell viability/ MTT assay

S10-3 human hepatoma cells were grown in Dulbecco's modified Eagle's medium (DMEM, Gibco/Thermo Fisher Scientific, cat. no. 31600034) supplemented with 10% (v/v) heat-inactivated fetal bovine serum (FBS; Gibco/Thermo Fisher Scientific, cat. no. 10099141), 100 U/ml of penicillin, and 100 µg/ml of streptomycin (MP Biomedicals, cat. no. 0916702-CF) at 37°C in a humid atmosphere saturated with 5% CO_2. For the MTT assay, cells were seeded in 96-well plates (10,000 cells/well) a day prior to the addition of drugs. Drugs were diluted in DMEM and added to cell monolayers, which were then incubated for 120 h. Cells were processed for measurement of toxicity using MTT reagent (thiazolyl blue tetrazolium bromide; Merck /Sigma-Aldrich, cat. no. M5655). The maximal nontoxic dose (MNTD) and half-maximal cytotoxic concentration (CC_{50}) were determined by nonlinear regression analysis in GraphPad Prism (version 8). Three sets of independent experiments were carried out, with each concentration tested in triplicate. The values obtained were normalized to the solvent control.

Testing of antiviral activity of drugs

In vitro transcription and capping

The HEV-1 subgenomic (SG) and full genomic (FG) replicon-encoding plasmids were linearized at the 3' end using BglII (New England Biolabs, cat. no. R0144], and the p6 HEV-3 SG replicon plasmid was linearized with MluI (New England Biolabs, cat. no. R0198), and these were used as templates to synthesize capped RNA using an mMESSAGE mMACHINE T7 ULTRA Transcription Kit (Thermo Fisher Scientific/Invitrogen, cat. no. AM1345). The DNA template was removed by DNase I treatment at 37°C for 15 min, and RNA was purified using the lithium chloride precipitation method. RNA was quantified using a NanoDrop ND-1000 spectrophotometer, (NanoDrop technologies), and its integrity was checked using denaturing 1% agarose gel electrophoresis.

Screening of drugs for anti-HEV-1 activity by luciferase assay

Primary screening of antiviral activity of the drugs was done using HEV-1 SG RNA harbouring the Rluc gene. The potential antiviral effect of the drug on HEV was tested at MNTD of the drug. Briefly, S10-3 cells (~10-15 × 10^5 cells) were seeded in a 25-cm^2 flask (Corning/Thermo Fisher Scientific, cat. no. 08-757-500) and allowed to grow for 24 h until reaching ~80% confluency. The next day, 15 µg of SG replicon RNA plus pGL4.75 hFluc/CMV plasmid DNA or firefly luciferase (FLuc) plasmid (100 ng/flask) diluted in OptiMEM Reduced Serum Medium (Gibco/Thermo Fisher Scientific, cat. no. 31985070) were mixed with 15 µl of 1,2-dimyristyl Rosenthal inhibitor ether C (DMRIE-C) transfection reagent (Invitrogen/Thermo Fisher Scientific, cat. no. 10459014) and added to the cells, which were then incubated at 34.5°C. The cells were co-transfected with FLuc plasmid DNA together with HEV SG RNA to normalize the cell transfection efficiency and the *Renilla* luciferase signal. Complete DMEM was added 4 h after transfection, and the cells were incubated at 34.5°C. After 48 h, the transfected cells were trypsinized, seeded into a 96-well plate, and further incubated for 24 h. Drugs were diluted in DMEM and added to the cells, which were then incubated further for 48 h. Mock-treated cells were incubated with 1% acetone (solvent control) for ART, whereas CQ, HCQ, and RBV are water soluble. Cells were harvested and lysed in 1X Passive Lysis Buffer (Promega, cat. no. E1980) and stored at -80°C until use. For measurement of reporter gene expression levels (*Renilla* luciferase activity), which correlates with the extent of HEV replication, cell lysates were thawed and centrifuged at 10,000 rpm for 2 min to remove cell debris, and the supernatant was used for measuring dual luciferase activity (Rluc and FLuc) using a Dual Luciferase Assay Kit (Promega, cat. no. E1980). Readings were taken on a Perkin Elmer Victor X3 Plate Reader Model 2030. Luminescence levels from drug-treated cells were compared with those of mock-treated cells, and the relative level of HEV replication was calculated. The half-maximal effective concentration (EC_{50}) of the drug was determined by using a twofold dilution series, starting with the half-maximal cytotoxic concentration (CC_{50}). EC_{50} values for drugs were calculated by

doing nonlinear regression in GraphPad Prism (version 8). Three sets of independent experiments were carried out in triplicate.

Immunofluorescence assay (IFA)

S10-3 cells were seeded in 6-well plates and transfected with pSK HEV-2 FG RNA (5 µg/well) after 24 h. Transfected cells were treated with RBV and ART at MNTD concentrations of 3.1µM and 23.4 µM, respectively. Cells were fixed and permeabilized with 90% acetone at -20°C for 20 min after 72 h and 96 h of transfection and washed twice with 1X PBST. Furthermore, cells were blocked with 20% FBS in PBST for 45 min at 37°C and washed five times with PBST and incubated with anti-HEV-IgG-antibody-positive human serum diluted 1:50 in PBST with 20% FBS for 1 h at room temperature (RT). After washing five times with PBST, the cells were incubated with goat anti-human IgG antibody-FITC conjugate (Merck/Sigma-Aldrich, cat. no. AP113F) at RT for 1 h and again washed five times with PBST. Cells were incubated with DAPI (Merck /Sigma-Aldrich, cat. no.10236276001) at RT for 2-3 min and then washed with PBST for removal of excess stain, mounted in 80% glycerol, and visualized using a FLoid Cell Imaging Station (Invitrogen).

ORF2 detection by western blot analysis

Cell pellets were lysed with RIPA buffer (Real Gene, cat. no. 150001), and soluble protein fractions (30 µg) were separated by 15% SDS-PAGE and transferred to a PVDF membrane (Millipore, cat. no. IPVH00010). The membrane was incubated with primary antibodies (anti-HEV mAb generated against a partial ORF2 protein containing amino acids 458 to 607)/anti-GAPDH antibody (Santa Cruz Biotechnology, cat. no. sc-365062). After washing three times with TBST buffer, the membrane was incubated with HRP-conjugated goat anti-mouse IgG antibodies (Bio-Rad, USA, cat. no. 1721011), and detection was done using Clarity™ Western ECL substrate (Bio-Rad, USA, cat. no. 1705060). The membrane was re-probed for detection of GAPDH as an internal control. Densitometric ratios were calculated by comparing the blot of the desired protein with GAPDH for accurate results using Gel Quant software, provided by BiochemLabSolutions.com.

Quantitation of HEV-1 RNA by reverse transcription quantitative polymerase chain reaction (RT-qPCR)

Drugs showing more than 30% inhibitory activity in the SG replicon culture system were further evaluated using the FG HEV replicon at MNTD concentrations of the drugs. The transfection protocol for the FG replicon was as follows: S10-3 cells were seeded in a 25-cm2 flask (10-15 $\times 10^5$ cells) and allowed to grow for 24 h. The next day, 15 µg of FG replicon RNA diluted in OptiMEM was mixed with 15 µl of DMRIE-C, added to the cells, and incubated at 34.5°C for 4 h. Complete DMEM was added 4 h after transfection, and the cells were incubated at 34.5°C for a further 48 h. After incubation, transfected cells were removed and seeded into 24-well plates and further incubated for 24 h. Drugs were diluted in DMEM and added to the cells, which were incubated further for 48 h. Mock-treated cells were incubated with the appropriate concentration of acetone (solvent control) for ART, whereas CQ, HCQ, and RBV are water soluble. After completion of the incubation period, the cell culture supernatant and cell pellets were harvested and stored at -80°C until further use. To quantitate cell-associated encapsidated viral RNA, cells were washed with 1X PBS and lysed with lysis buffer (10 mM Tris-HCl, pH 7.5, 50 mM NaCl, 1 mM EDTA, 0.25% NP-40, and 8% sucrose) as described previously [54]. Similarly, virus particles released in the cell culture supernatant were lysed with lysis buffer. To quantitate intracellular and extracellular viral RNA from cell pellets and cell culture supernatant, respectively, virus particles were precipitated by adding polyethylene glycol 6000 as described previously [55]. Both the cell lysate and the solubilized PEG precipitates were treated with DNase

Table 1 Inhibitory activity of drugs against HEV-1 and HEV-3

Drug	CC_{50} (µM)	EC_{50} (µM) for HEV-1	TI for HEV-1	HEV-1 inhibition (%)	HEV-3 inhibition (%)
RBV	39 ± 5.9	2.9 ± 0.53	6.38	62 ± 7	46 ± 5
ART	189 ± 14.11	19.5 ± 4.03	9.68	59 ± 6	43 ± 5
CQ	4.77 ± 0.74	-	-	23 ± 2	ND
HCQ	4.1 ± 0.052	-	-	9 ± 1.4	ND
RTP	169 ± 1.6	7 ± 0.2			ND

CC_{50}, half-maximal cytotoxic concentration; EC_{50}, half-maximal effective concentration; TI, therapeutic index (CC_{50}/EC_{50}); ND, not determined

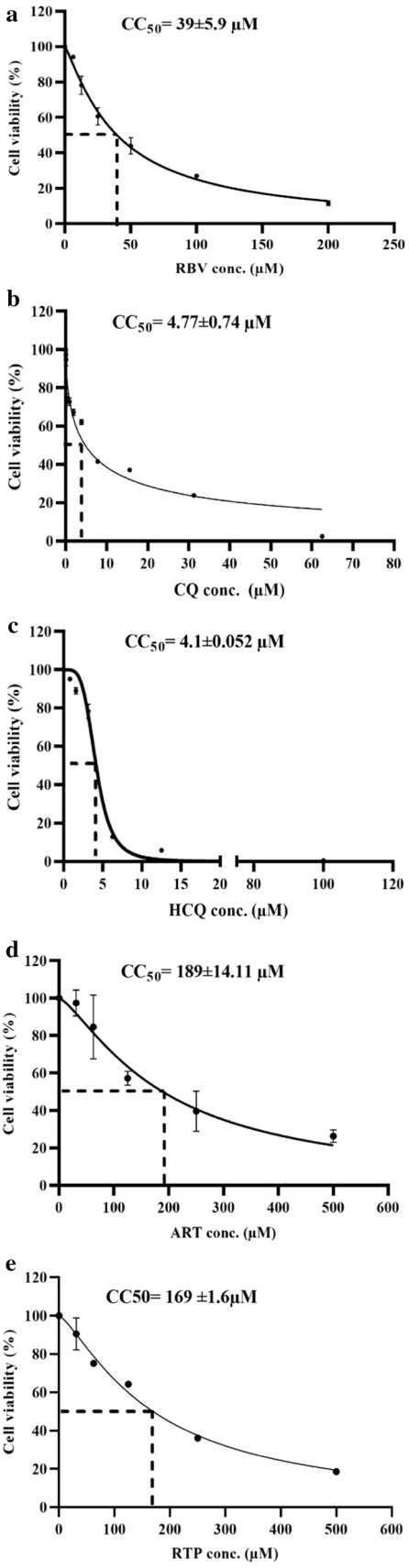

Fig. 1 Cell cytotoxicity assay to determine CC_{50} values. The effect of drugs on S10-3 cell viability was determined using MTT assay. Cells were exposed to different concentrations of drugs for 120 h and processed for colorimetric measurements. (a) RBV (R^2 = 0.98), (b) CQ (R^2 = 0.94), (c) HCQ (R^2 = 0.99), (d) ART (R^2 = 0.91), (e) RTP (R^2 = 0.93). CC_{50} values were determined using GraphPad Prism. Three sets of independent experiments were carried out in triplicate for the CC_{50} estimation.

I (500 µg/ml) and RNase A (100 µg/ml) at 37°C for 30 min to digest free replicon RNA and plasmid DNA (if present) and processed for viral RNA extraction using a QIAamp Viral RNA Mini Kit (QIAGEN, cat. no. 52906). HEV RNA levels were measured using TaqMan MGB probe primers on a 7300 Real-Time PCR system (Applied Biosystems, USA) as described earlier [56]. HEV-specific primers were used for quantitation of encapsidated viral RNA copies targeting ORF1, which consisted of a forward primer (HEV-1 SET2F- AGTGCTYGACCTGAC AAATTC-AAT; 5065-5088), a reverse primer (HEV-1 SET2R- GGCGCAGCARAAGACATGTT; 5110-5129), and a probe (FAM- 5'TCGGGTGGAATGAA3'-MGB). The thermal cycling protocol used was as follows: stage 1, 48°C for 30 min; stage 2, 95°C for 10 min; stage 3, 45 cycles of 95°C for 15 s and 60°C for 1 min. HEV-FG RNA was serially diluted to obtain 10^8 to 10 copies and used as an external standard for calculating RNA copy numbers in the samples. For normalization, the average number of HEV RNA copies in the cell supernatant and cell pellet, harvested at 48 h post-transfection, were taken as baseline/input RNA copy numbers and subtracted from the respective values of the samples. Mean values were calculated from three sets of independent experiments carried out in triplicate.

Screening of drugs for anti-HEV-3 activity by luciferase assay

Drugs showing promising inhibitory activity against HEV-1 were also tested against HEV-3 using a subgenomic (SG) replicon. Transfection of S10-3 cells with HEV-3 SG RNA was done as described above for the HEV-1 SG replicon in a 25-cm^2 flask. Cells were co-transfected with firefly luciferase (FLuc) plasmid DNA together with HEV-3 SG RNA to normalize the cell transfection efficiency and the *Renilla* luciferase signal. Drugs were diluted in DMEM and added to cells. Mock-treated cells were incubated with the appropriate concentration of acetone (solvent control) for ART, whereas RBV is water soluble. Dual luciferase activities (Rluc and FLuc) were determined using a Dual Luciferase Assay Kit. Final readings were taken on a Perkin Elmer 2030 Reader, and luminescence levels from drug-treated cells were compared with mock-treated cells to determine relative HEV

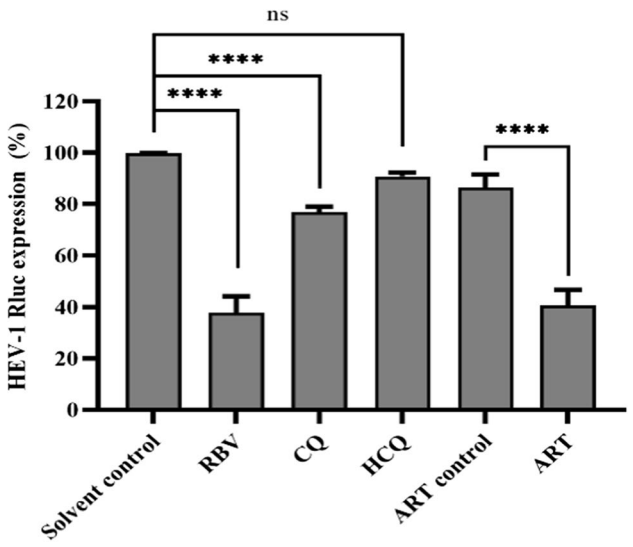

Fig. 2 Evaluation of inhibitory effects of drugs against HEV-1. Drugs were evaluated for antiviral activity against HEV-1 using a subgenomic-replicon-based culture system at the maximum nontoxic doses of RBV (3.12 µM), CQ (0.06 µM), HCQ (0.78 µM), and artesunate (23.43 µM). HEV replication in cells was assessed by dual luciferase assay. The HEV-1 replication in the solvent control was taken as 100% to calculate percent HEV inhibition. *, $P < 0.05$; **, $P < 0.01$; ***, $P < 0.001$; ****, $P < 0.0001$. Data are expressed as mean values ± SD. Mean values were calculated from three sets of independent experiments carried out in triplicate.

replication. Mean values were calculated from three sets of independent experiments carried out in triplicate.

Helicase model building with SWISS-Model server and molecular docking

Since three-dimensional (3D) crystallographic structure of the HEV helicase domain is not available in the Protein Data Bank (PDB), it was predicted using the online Swiss-Model server (https://swissmodel.expasy.org/interactive). 3WRX.pdb (crystal structure of tomato mosaic virus helicase complex) was used as a template. This structure has a resolution of 2.5Å, and its sequence is 32% identical to the HEV sequence. The quality of the modelled structure was assessed by generating a Ramachandran plot using the PROCHECK module on the SAVES server (https://saves.mbi.ucla.edu/).

The ligand-protein docking interactions of the modeled HEV helicase structures were simulated using AutoDock Vina. The 2-D structures of ligands such as artesunate were downloaded from PubChem (https://pubchem.ncbi.nlm.nih.gov/) and preprocessed using AutodockTool (ADT) for further docking studies. The HEV helicase structure was also preprocessed and minimized by adding polar hydrogens and Gasteiger charges using ADT. The

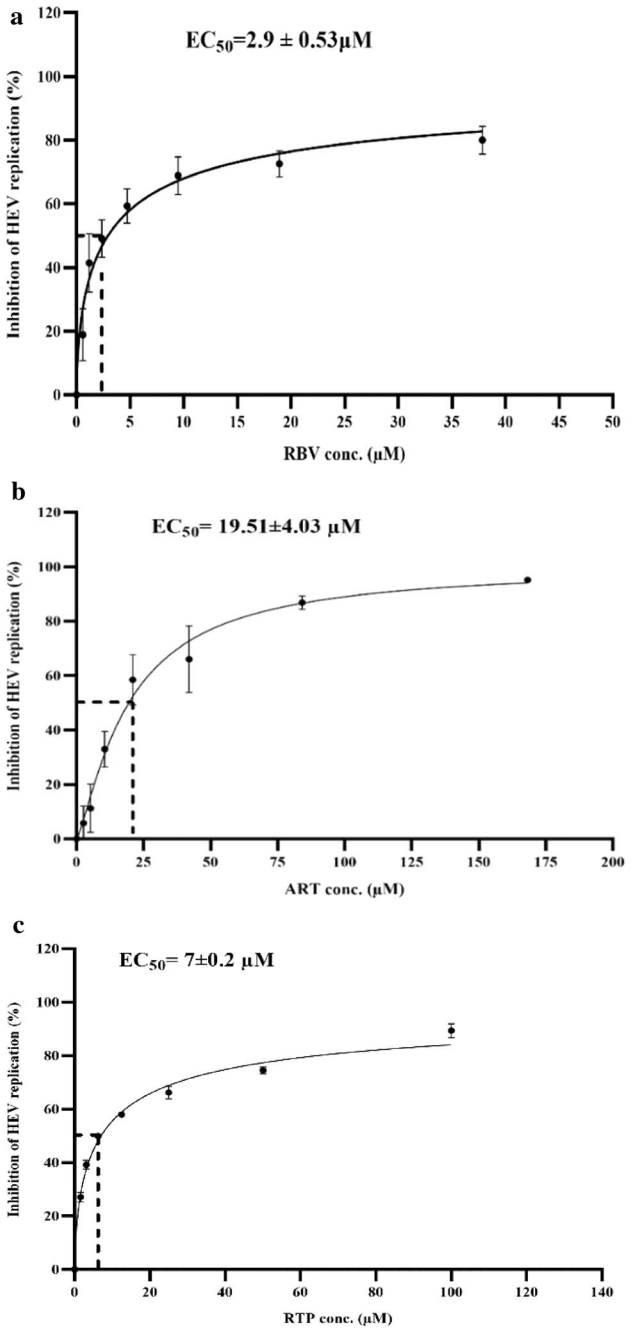

Fig. 3 Determination of EC_{50} values for RBV and ART. A twofold dilution series of drugs was tested against HEV-1 using a subgenomic replicon system for determination of EC_{50} values. (a) RBV (R^2 = 0.94), (b) ART (R^2 = 0.96), (c) RTP (R^2 = 0.98). EC_{50} values were determined using GraphPad Prism software. Each experiment was repeated three times in triplicate.

grid box parameters were set in such a way that the search was performed over the entire protein surface. Default values were used for all other docking parameters. The binding site predictions prior to docking studies, the interaction analysis, and molecular visualization of docked

complexes were performed using the BIOVIA Discovery Studio 2020 client software package.

Purification of the helicase protein and ATPase assay

The HEV helicase domain (amino acids 960 to 1204 of HEV-1 ORF1) clone pET15b.HEV Hel was constructed previously in our laboratory [57]. BL21-CodonPlus (DE3)-RIL competent cells (Agilent Technologies, cat. no. 230245) were transformed with the plasmid, and induction was done with 1.0 mM IPTG for 4 h at 37°C. The N-terminal His tag fusion protein was purified from bacterial culture pellets as described earlier [58]. Fractions containing the desired protein were analyzed by 10% SDS-PAGE and further purified by dialysis in 50 mM HEPES buffer for 1-2 h. Western blot analysis was done using anti-HIS mAbs (Sigma-Aldrich, cat. no. SAB2702218-100UL). The protein concentration was determined by the Bradford method.

ATPase assays were performed by using a colorimetric method described earlier [58]. For testing the effect of drugs on the enzyme, the helicase protein was incubated with the stipulated concentration of drugs for 30 min before the assay. The ATPase activity of the protein was assayed in a 50-µl reaction containing 300 pmol of purified protein, 50 mM HEPES (pH 7.2), 2 mM $MgCl_2$, 10 mM KCl, 0.05 mg of BSA per ml, 2 mM dithiothreitol (DTT), and 100 µM ATP, with incubation at 37°C for 40 min. Colour was developed by adding an equal volume of malachite green molybdate reagent, followed by incubation at room temperature for 30 min and absorbance measurement at 630 nm in a µQuant 96-well plate reader (Bio-Tek). Mean values from three independent experiments performed in triplicate were calculated. ATPase activity was measured as the amount of inorganic phosphate released by ATP hydrolysis, and a standard curve was plotted with known concentrations of potassium dihydrogen phosphate. Relative activity was calculated by taking the ATPase activity of helicase in the presence of the respective drug solvents as 100%.

Expression and purification of the HEV RdRp protein and polymerase assay

The recombinant plasmid pET28a.HEV RdRp, encoding the HEV RdRp domain encompassing all (A-H) conserved motifs of the protein (510 amino acids, aa 1199-1709 of the HEV ORF1 polyprotein; HEV-1, GenBank accession no. AF444002) was available in our laboratory. BL21-CodonPlus (DE3)-RIPL competent cells (Agilent Technologies, cat. no. 230280) were transformed with the above recombinant plasmid, and induction was done with 0.5 mM IPTG and 5 mM $MgCl_2$ for 16 h at 28°C. The N-terminal His tag fusion protein was purified from bacterial culture pellets using an Ni-NTA purification system (Thermo Fisher Scientific/Invitrogen, cat. no. K95001) under native conditions. Briefly, the induced cell pellet (500 ml) was lysed in 15 ml of native binding buffer (50 mM NaH_2PO_4, pH 8.0, 0.5 M NaCl, 10 mM imidazole, and 5 mM $MgCl_2$) containing a 1X protease inhibitor mix (Merck/Roche, cat. no. 11873580001) and 16 mg of lysozyme (Sigma-Aldrich/ Merck, cat. no. L6876). Cells were kept on ice for 30 min and then sonicated with 10-s on-off cycles for 20 min on ice. The cell lysate was treated with DNase I (200 Kunitz units; MP Biomedicals, cat. no. 02100575-CF) and RNase A (70 Kunitz units; Sigma Aldrich/Merck, cat. no. R6513) for 30 min and centrifuged at 12,000 rpm for 30 min at 4°C, and the supernatant was loaded onto an Ni-NTA resin affinity column. Binding of the desired proteins to the resins was carried out for 1.5 h on ice, and unbound proteins were removed using 30 ml of native wash buffer (50 mM NaH_2PO_4, pH 8.0, 0.5 M NaCl, 5 mM $MgCl_2$] with 10 mM imidazole and 15 ml of native wash buffer (50 mM NaH_2PO_4, pH 8.0, 0.5 M NaCl, and 5 mM $MgCl_2$) with 20 mM imidazole. The desired protein was eluted in native elution buffer (50 mM NaH_2PO_4, pH 8.0, 0.5 M NaCl, 5 mM $MgCl_2$) with 100 mM imidazole. Fractions were analyzed by SDS-PAGE, and those containing a 56-kDa protein were pooled, concentrated, and exchanged into HEPES buffer (50 mM HEPES [pH 7.4], 500 mM NaCl, and 5 mM $MgCl_2$) using Amicon ®Ultra-15 Centrifugal Filter Units (cutoff, 10 kDa; Merck/ Millipore, cat. no. UFC9010). Protein was further purified by size exclusion chromatography using Superdex® 200 Increase 10/300 GL (Sigma-Aldrich/ Cytiva 28-9909-44, cat. no. GE28-9909-44), using an AKTA Basic 100 HPLC System (Amersham Pharmacia). The final purified protein was analyzed by 10% SDS-PAGE and confirmed by western blot using anti-His mAb (Sigma-Aldrich, cat. no. H1029), quantitated by the Bradford method, and stored in aliquots at -20°C until further use.

The colorimetric RdRp assay was carried out using malachite green dye. The 50 µl reaction mixture contained 50 mM HEPES, pH 7.4, 5 mM $MgCl_2$, 4 mM DTT, 10 µg of BSA per ml, 2.5 mM rNTPs, and 0.5 µM enzyme, along with the desired concentration of the drug and 20 U of RNasin (Promega, Cat No. N2111). The reaction mixture was incubated at 37°C for 30 min to remove any contaminating RNase, and 5 U of thermostable inorganic pyrophosphatase (NEB, cat. no. M0296) and 0.5 µM of *in vitro*-synthesized 3'NCR HEV RNA template were added as described previously [59]. The polymerization reaction was carried out at 30°C for 2 h. The reaction mixture was kept at 70°C for 30 min to inactivate the enzymes. Colour was developed by adding 100 µl of malachite green-molybdate reagent, followed by incubation at room temperature for 30 min and absorbance measurement at 630 nm on a µQuant 96-well plate reader (Bio-Tek). Mean values of three independent experiments performed in triplicate were obtained to calculate the polymerase activity

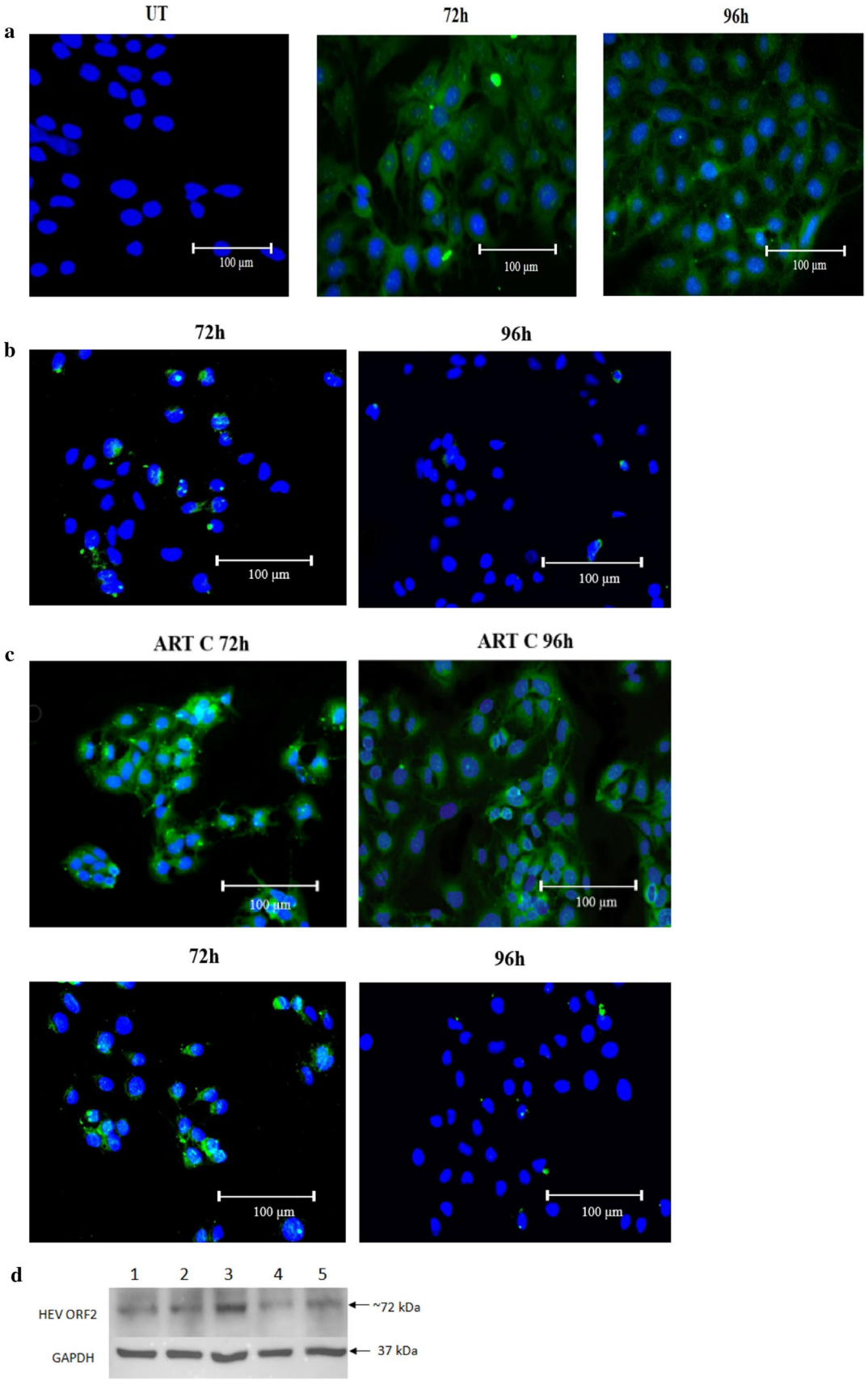
a
UT
72h
96h
100 µm
b
72h
96h
100 µm
c
ART C 72h
ART C 96h
100 µm
d
1 2 3 4 5
HEV ORF2
GAPDH
~72 kDa
37 kDa

◂**Fig. 4** Assessment of ORF2 expression in transfected cells. S10-3 cells were transfected with an HEV-1 full-genomic replicon and treated with RBV or ART. Cells containing (a) no drugs, (b) RBV, and (c) ART were fixed at 72 h and 96 h post-transfection and processed for immunofluorescence assay using anti-HEV-IgG-positive human serum as primary antibody and goat anti-human IgG-FITC conjugate as secondary antibody. Nuclei were counterstained with DAPI for fluorescence microscopy. Expression of ORF2 protein could be observed at the perinuclear region of cells. UT, untransfected cells; ART C, solvent control for ART. (d) Western blot analysis of cell pellets for detection of HEV ORF2 using anti-ORF2 monoclonal antibodies. Lane 1, RBV 72 h; lane 2, RBV 96 h; lane 3, ART C (solvent control); lane 4, ART 72 h; lane 5, ART 96 h

based on the amount of inorganic phosphate released. A standard curve was prepared with known concentrations of potassium dihydrogen phosphate. The relative activity was calculated by taking the polymerase activity of RdRp in the presence of the respective drug solvents as 100%.

Statistical analysis

Data are expressed as the mean ± standard deviation of three sets of experiments carried out in triplicate. Statistical analysis was carried out using Excel for Windows, and statistical comparison of means was performed by using Student's *t*-test after analysis of variance. Differences were considered statistically significant at $p < 0.05$. Graphs were plotted using GraphPad Prism 8.0 software for Windows.

Results

CC_{50} determination and evaluation of antiviral activity of drugs against HEV-1

S10-3 human hepatoma cells were treated with RBV, CQ, HCQ, and ART to determine the MNTD and CC_{50} using an MTT assay. RBV, a drug that is currently used for the treatment of hepatitis E, was included as a control in all cell culture experiments. The CC_{50} values for RBV, CQ, HCQ, ART, and RTP were found to be 39 ± 5.9 µM 4.77 ± 0.74 µM, 4.10 ± 0.05 µM, 189 ± 14.11 µM and 169 ± 1.6 µM, respectively (Table 1), while the MNTDs of these drugs were 3.12 µM, 0.06 µM, 0.78 µM, 23.43 µM, and 7.8µM, respectively (Fig. 1 a-e).

Primary-level evaluation of antiviral activity was done at the MNTD of the drugs, using a subgenomic replicon culture system (HEV-1 SG), since it enabled quantitative assessment of HEV replication directly by measurement of Rluc activity. A known inhibitor of HEV, RBV, was used as a reference control in all HEV inhibition experiments [60]. RBV, CQ, HCQ, and ART showed 62%, 23%, 9%, and 59% inhibition of HEV replication, respectively (Fig. 2). Since CQ and HCQ showed little inhibition at the MNTD, EC_{50} values could not be calculated for these drugs. The EC_{50} values estimated for RBV, ART, and RTP were 2.9 ± 0.53 µM, 19.51 ± 4.03 µM, and 7 ± 0.2 µM, respectively. RBV, ART, and RTP exhibited a dose-dependent increase in the inhibition of HEV replication, as evaluated by *Renilla* luciferase activity (Fig. 3a-c and Table 1).

Evaluation of the inhibitory activity of RBV and ART using an HEV-1 full-genome replicon culture system

The inhibitory activity of RBV and ART was confirmed using an HEV-1 FG replicon because the subgenomic replicon is not able to synthesize functional ORF2 and ORF3 proteins, which are required for encapsidation and release of virus. The FG replicon undergoes a complete replication cycle with the release of virions. To compare the antiviral activity of these drugs in the two viral replicon culture systems, S10-3 cells were transfected with HEV-1 FG RNA and treated with drugs. HEV replication was confirmed by detecting the expression of the ORF2 (capsid) protein by immunofluorescence assay. ORF2 protein expression could be seen at 72 h post-transfection, with a significant further increase at 96 h post-transfection (Fig. 4a). Treatment of cells with RBV and ART showed decreased ORF2 levels after 72 h and 96 h (Fig. 4b and c). A decrease in ORF2 levels was also evident from western blot analysis (Fig. 4d). For quantitative estimation of the effectiveness of drugs against HEV, a real-time RT-PCR assay was used to quantitate HEV RNA. To avoid error due to carryover contamination with the viral RNA used for cell transfection, only encapsidated HEV was used to estimate the RNA copy numbers. The average number of HEV RNA copies in the cell supernatant and cell pellet harvested 48 h post-transfection was taken as the baseline/input RNA copy number, and this was subtracted from the values obtained at later time points to estimate the number of encapsidated HEV RNA copies. Both RBV and ART were tested at the MNTD: 3.1 µM and 23.4 µM, respectively. Interestingly, RBV treatment resulted in an 84% reduction in the number of HEV RNA copies in cells and a 92% reduction in supernatant, while ART treatment resulted in an 81% and 69% reduction, respectively (Fig. 5a and b and Table 2). The therapeutic indices (CC_{50}/EC_{50}) for RBV and ART were 6.38 and 9.68, respectively. Thus, compared to the SG replicon, the FG replicon culture system showed significantly higher levels of inhibition of production of cell-free and cell-associated virions by both RBV and ART. The data suggest that ART is a potent inhibitor of HEV-1 replication. Since a significant inhibitory effect of ART was also evident in the subgenomic culture system, this effect might be due to

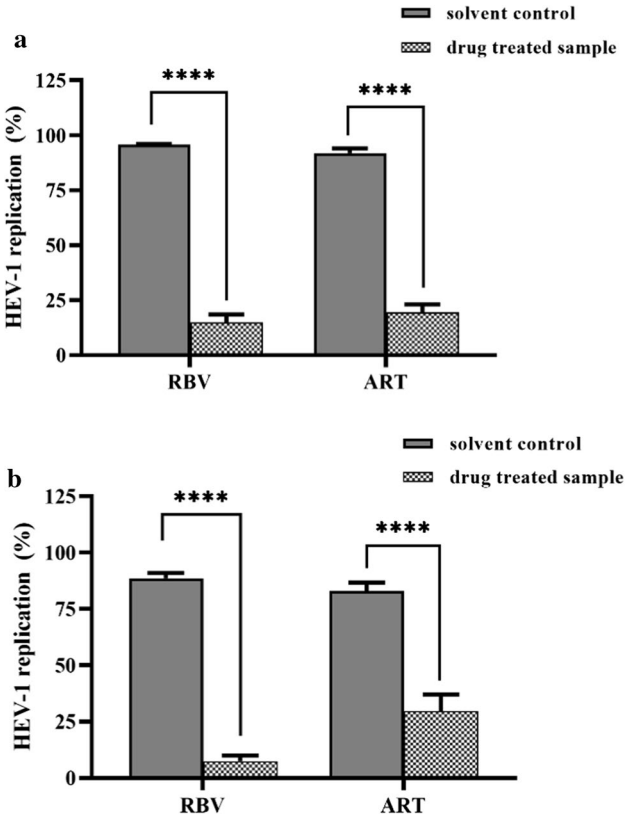

Fig. 5 Comparative inhibitory effect of RBV and ART evaluated using the HEV-1 full-genome replicon. S10-3 cells were transfected with the HEV-1 full-genomic replicon, incubated for 72 h, and then treated with RBV (3.12 µM) or ART (23.43 µM) for 48 h. Both cell supernatants and cells were processed for HEV RNA estimation using real-time PCR. For normalization, the average number of HEV RNA copies in the cell supernatant and cell pellet harvested at 48 h post-transfection were taken as the baseline/input RNA copy numbers and subtracted from the respective values to calculate final HEV RNA copy numbers. (a and b) HEV RNA levels in (a) cell pellets and (b) culture supernatants. *, $P < 0.05$; **, $P < 0.01$; ***, $P < 0.001$; ****, $P \leq 0.0001$. Data are expressed as mean values ± SD. Mean values were calculated from three sets of independent experiments carried out in triplicate.

Table 2 Inhibition activity measured using a real-time PCR assay

Drug	MNTD (µM)	HEV-1 inhibition (%)	
		Cell pellet	Cell supernatant
RBV	3.1	84 ± 3.7	92 ± 2.5
ART	23.4	81 ± 3.8	69 ± 7.3

MNTD, maximum nontoxic dose, the highest concentration of drug tolerated by S10-3 cells

inhibition of viral enzymes or cellular factors that play important roles in HEV RNA replication.

To assess the effect of ART on HEV-3 replication, an HEV-3 subgenomic-replicon-based culture system was used.

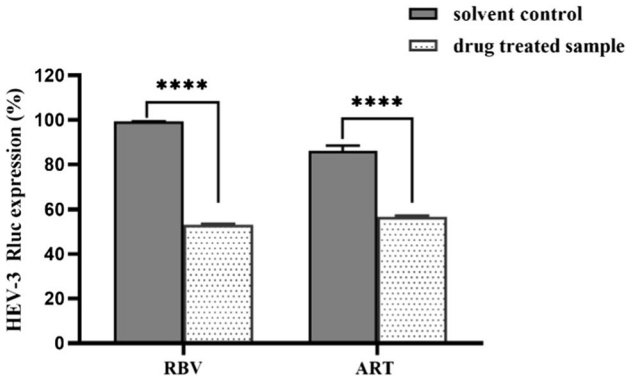

Fig. 6 Evaluation of the inhibitory effect of ART against HEV-3. S10-3 cells were transfected with the HEV-3 subgenomic replicon, incubated for 72 h, and then treated with RBV (3.12 µM) or ART (23.43 µM) for 48 h. HEV replication in cells was assessed by dual luciferase assay. The luciferase activity obtained with the solvent control was taken as 100% to calculate percent inhibition in drug-treated cells. *, $P < 0.05$; **, $P < 0.01$; ***, $P < 0.001$; ****, $P < 0.0001$. Data are expressed as mean values ± SD. Mean values were calculated from three sets of independent experiments carried out in triplicate.

Interestingly, ART treatment resulted in a 43% reduction in Rluc activity, while RBV treatment resulted in a 46% reduction. This shows that ART is also effective against HEV-3 (Fig. 6 and Table 1).

Molecular docking of ART on the HEV helicase protein

To assess whether ART might interact with the HEV helicase and RdRp proteins, which are the key enzymes involved in HEV RNA replication, we used a computational approach. Galani et al. [38] have reported that artemisinin, the parent molecule of ART, has low binding affinity to HEV RdRp; hence, we focused on HEV helicase. As there was no crystal structure of HEV helicase in the PDB database, the 3-D structure was predicted using tomato mosaic virus (ToMV) helicase, which has 32% sequence identity, as a template. Both ToMV and HEV are members of the alpha-like supergroup of positive-sense RNA viruses and possess superfamily 1 helicases (Fig. 7a). The quality of the predicted structure was evaluated by Ramachandran plot analysis (Fig. 7c), which showed a good-quality structure, with 89% of the residues lying within the most-allowed region and 9.1 and 1.1% of the residues lying in the additionally allowed and generously allowed regions, respectively. The HEV helicase protein has multiple binding sites, but the most prominent and crucial site is the ATP binding site, as this provides energy via hydrolysis of ATP for the unwinding activity of the enzyme (Fig. 7b). The ATP binding site involves multiple motifs, including the Walker A motif (975-GVPGSGKSRS-985), the Walker B motif

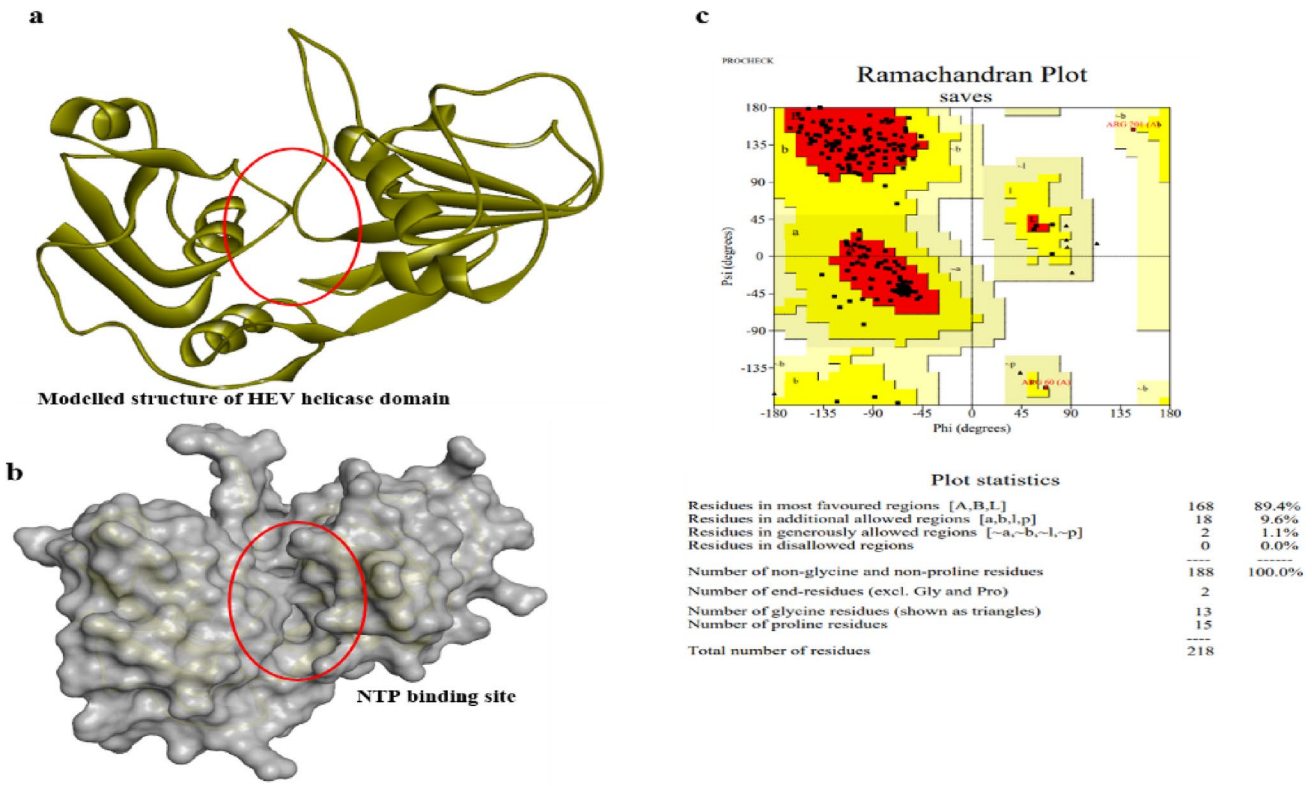

Fig. 7 HEV helicase protein structure predicted using the Swiss-Model server. (a and b) Three-dimensional modeled structure of the HEV helicase domain shown (a) in ribbon form and (b) as a surface-rendered view with the NTP binding site highlighted. (c) Ramachandran plot analysis of the modeled structure

(1029-GRRVVIDEAP-1038), and motif III (1051-HLLG-DPNQ-1058). The docking interaction of ART with HEV helicase showed good binding, with an affinity score of -7.4 kcal/mol (Fig. 8c). ART was predicted to interact well with HEV helicase, with three hydrogen bonding interactions with the Walker A motif residues Gly 979, Lys 982, and Ser 983, and it was also predicted to interact with Arg 984 via van der Waals interactions (Fig. 8d). In comparison, ATP formed multiple hydrogen bonds with motif A residues, with a binding affinity of -8.9 kcal/mol (Fig. 8a and b). Despite ART having a lower docking score than ATP, which might be due to lower site occupancy and solvent accessibility, ART was predicted to bind to crucial residues of the Walker A motif that could hinder the ATP hydrolysis function of the helicase and ultimately inhibit the viral replication process.

Inhibition of the ATPase activity of HEV-1 helicase by ART

To test whether ART indeed inhibits the ATP hydrolysis activity of HEV helicase, a recombinant HEV-1 helicase protein was used. The protein was expressed with an N-terminal histidine tag in a bacterial expression system, purified using nickel affinity chromatography under denaturing conditions, and refolded in renaturation buffer. Renatured protein was dialysed in 50 mM HEPES, pH 7.2, for 1-2 h. The dialysed protein (28 kDa) was analyzed by 10% SDS-PAGE (Fig. 9a) and western blot analysis (Fig. 9b). For the ATP hydrolysis assay [58], the helicase protein was pre-incubated with different concentrations of ribavirin triphosphate (RTP) (3.5 to 56 µM) and ART (4.8 to 156 µM) for 30 min, and its hydrolysis activity was measured using 100 µM ATP as a substrate. For all *in vitro* studies, instead of ribavirin, ribavirin triphosphate was used as a control. The ATPase activity of the helicase in the solvent control samples, measured in the form of PO_4 release, was found to be 5551 ± 86 pmol and 5404 pmol, which was considered 100% activity for ART and RTP, respectively. On pre-incubation of helicase with 7 µM RTP (EC_{50}), there was a 16% reduction in ATPase activity. Surprisingly, a reduction of 22% in the activity was observed with a lower (3.5 µM) concentration of RTP (Fig. 9c). Pre-incubation of helicase with 19.5 µM ART (EC_{50}) resulted in a 24% reduction in activity, and a similar reduction (23%) was observed at a lower concentration (4.8 µM). With increasing ART concentration, there was a proportionate decrease in the enzymatic activity up to 78 µM (~55% reduction) (Fig. 9d). These results support

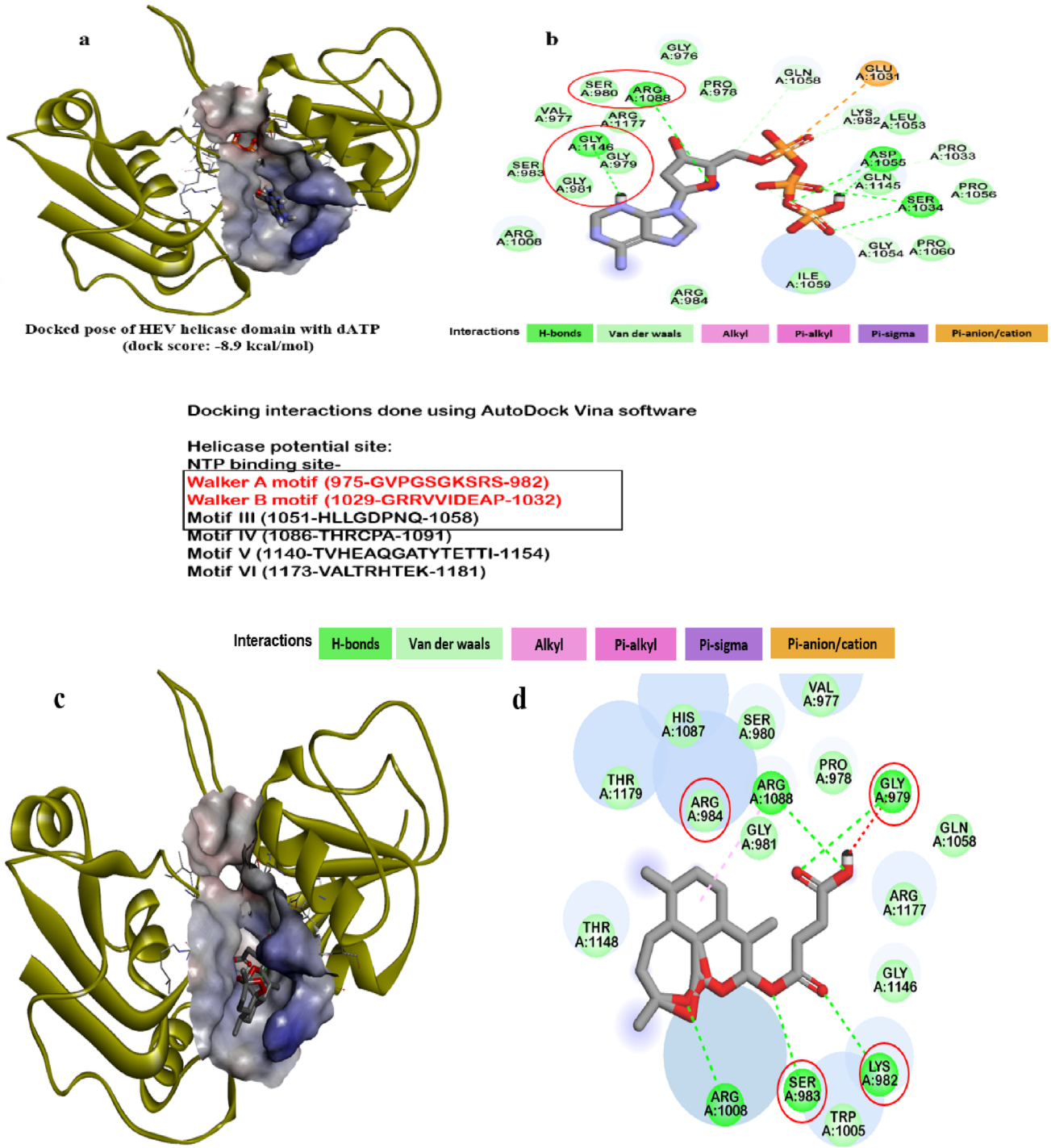

Fig. 8 Docking interaction analysis of ATP and ART with the HEV helicase domain. (a and b) 3D and 2D interaction of the HEV helicase domain with ATP. (c and d) 3D and 2D interaction of the HEV helicase domain with ART. The docking site (NTP binding site) is shown as a surface-rendered view and coloured by interpolated charge.

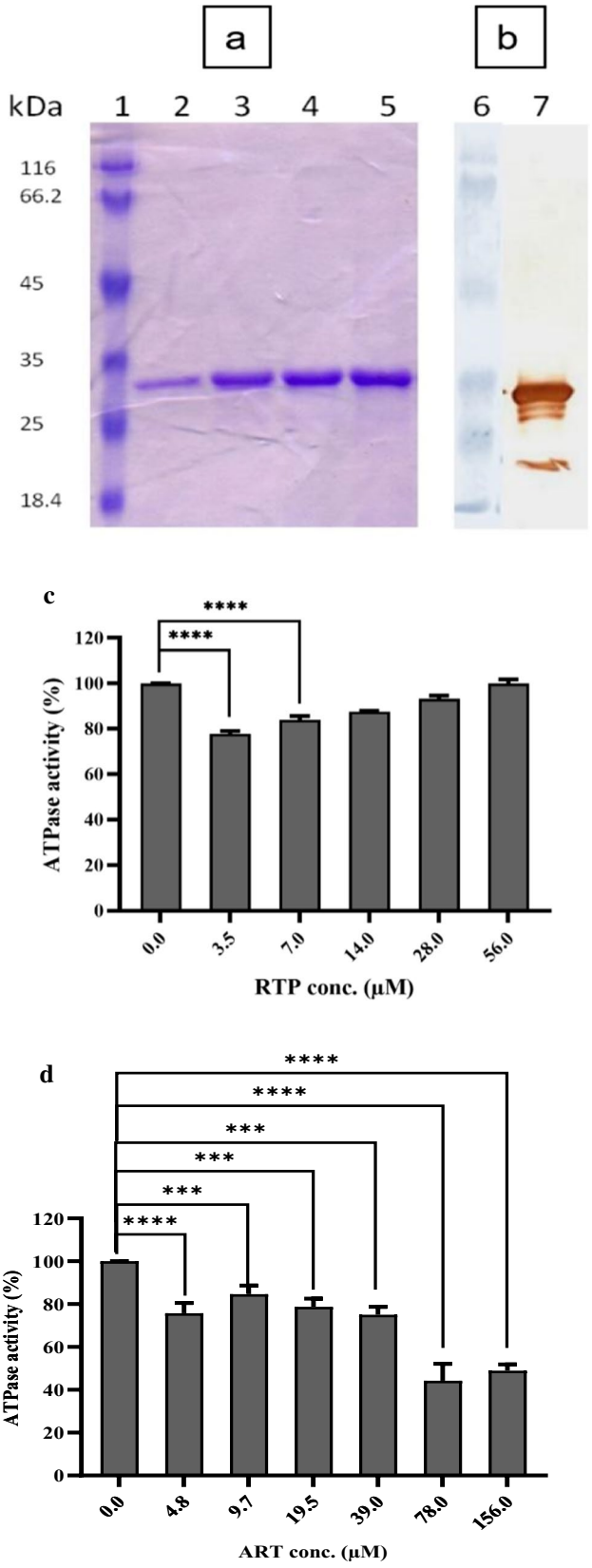

Fig. 9 Determination of the ATPase activity of HEV-1 helicase in the presence of drugs. (a) HEV-1 helicase protein was purified by Ni-NTA chromatography, and fractions containing a protein of the expected size (28 kDa) were analysed by 10% SDS-PAGE with Coomassie brilliant blue staining. Lane 1, protein molecular weight marker (Fermentas SM0431); lanes 2-5, protein purified with Ni-chelating resin and dialyzed in 50 mM HEPES. (b) HEV-1 helicase protein was separated by 10% SDS-PAGE, transferred to a nitrocellulose membrane, and detected using anti-his antibody. Lane 6, protein molecular weight marker; lane 7, helicase protein dialyzed in 50 mM HEPES, pH 7.2. The ATPase activity of the helicase protein was evaluated in the presence of different concentrations of (c) RTP and (d) ART. The enzyme was pre-incubated with different concentrations of the drugs for 30 min, followed by ATPase assay. The enzymatic activity of the helicase protein without drug treatment was considered 100%, and the percent inhibition at different RTP and ART concentrations was calculated. Each drug concentration was tested in triplicate in three independent experiments.

the molecular docking predictions that ART interacts with HEV helicase to inhibit ATPase activity.

Mechanism of inhibition of helicase by ART

To investigate whether there is competition for the helicase binding site between ART and ATP, the HEV helicase protein was pre-incubated with a fixed concentration of ART (EC_{50}: 19.5 μM) for 30 min and assayed for ATPase activity by adding different concentrations of the substrate ATP (from 50 to 500 μM), keeping other reaction conditions constant. In parallel, a control set of reactions was carried out with varying ATP concentrations without ART for comparison. As expected for the control reactions, with an increase in ATP concentration from 50-300 μM, the enzyme showed an increase in ATPase activity from 90% to 100%, while enzymatic activity decreased with a further increase in ATP above 300 μM. Importantly, pre-incubation with 19.5 μM ART resulted in a significant decrease in activity at 50 μM ATP, from 93% in the control reaction to 62% with ART. Interestingly, a further increase in the ATP concentration from 100 to 400 μM resulted in a gradual increase in ATPase activity up to 80%. However, the enzymatic activity did not reach to its 100% level (V_{max}) in the presence of ART even with higher concentrations of substrate ATP, indicating that, when the enzyme is pretreated with ART, ART behaves as a noncompetitive inhibitor (Fig. 10a).

To investigate whether pre-incubation of the enzyme with the substrate ATP has the ability to overcome the effect of ART, assays were carried out by incubating the enzyme with different concentrations of ATP for 30 min prior to the addition of 19.5 μM ART. Pretreatment with ATP resulted in higher ATPase activity when compared to pretreatment with ART. At 50 μM ATP, the ATP-pretreated enzyme showed ~79% activity, whereas the ART-pretreated enzyme showed 62% activity. At 100 μM ATP, these values were 86% and 75%, respectively. With higher ATP concentrations, the

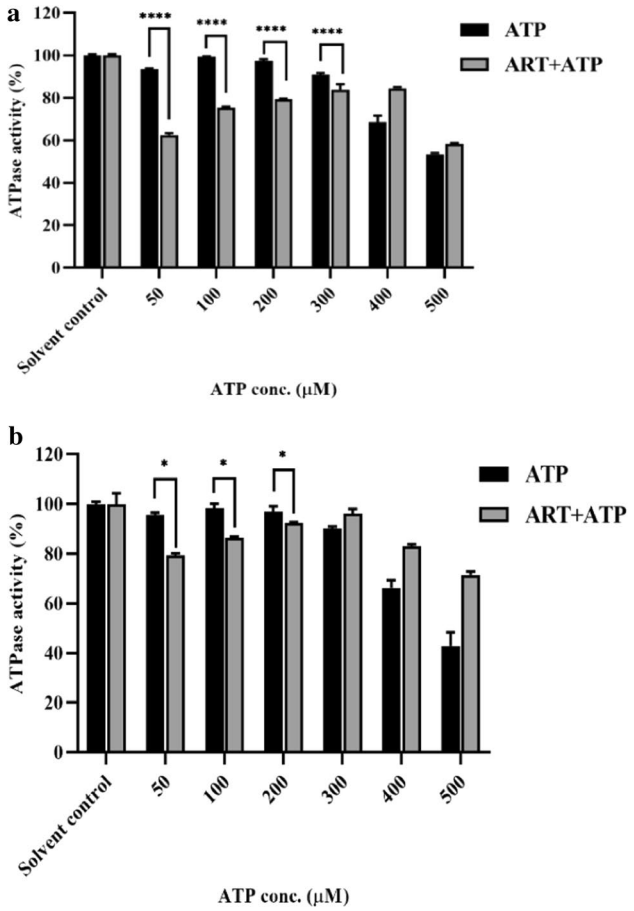

Fig. 10 Determination of the mode of action of ART on the ATPase activity of HEV-1 helicase. ATPase assays were performed in the presence of ART with different concentrations of the substrate ATP. (a) The helicase protein was pre-incubated with (19.5 μM) ART for 30 min and processed further for ATPase assay. (b) The helicase protein and ATP were pre-incubated for 30 min before addition of ART and processed further for ATPase assay. All assays were done in triplicate in three independent experiments.

ATP-pretreated enzyme showed 100% activity, comparable to the control set. Thus, a higher concentration of the substrate (200 μM ATP) was required in the presence of ART to achieve 100% activity of the enzyme (V_{max}), indicating that ART behaved as a competitive inhibitor in the ATP pretreatment assay (Fig. 10b).

These observations clearly indicate that there is direct competition between ART and ATP for binding to the ATP-binding site of the helicase protein. With higher binding affinity, ATP competed well with ART, and with prior addition it probably blocked the active site of the enzyme and prevented the binding of ART. However, pre-incubation of the enzyme with ART in the absence of ATP allowed it to bind to the active site. ATP was probably able to bind to the enzyme-ART complex but was not able to completely rescue the enzyme activity, since ART also has affinity for the site and presumably remained bound to the enzyme to hinder efficient ATP hydrolysis. Overall, it appears that the inhibition of helicase by ART is reversible.

Inhibition of the polymerase activity of HEV-1 RdRp by ART

Recombinant HEV-1 RdRp protein was used to determine whether ART has an inhibitory effect on the polymerase activity of this enzyme. RdRp with an N-terminal histidine tag was expressed in a bacterial expression system and purified using nickel affinity chromatography under native conditions. Further purification of the protein was carried out using size exclusion chromatography, and it was finally eluted in HEPES buffer. The purified protein (56 kDa) was analyzed by 10% SDS-PAGE (Fig. 11a) and western blot analysis (Fig. 11b). RTP has been reported previously to inhibit HEV replication by binding to RdRp protein [31, 61]. A polymerase inhibition assay was performed by incubating RdRp with different concentrations of ART (4.8 to 78 μM) and measuring the activity of the enzyme in the form of PO_4 release, by colorimetric assay. The enzyme activity obtained with RTP solvent control (8547 ± 235 pmol) was taken as 100% activity when measuring the inhibitory effect of RTP. At 7 μM RTP (EC_{50}), a 20% reduction in the polymerase activity was seen, which increased further to a maximum of 28% with an increase in the RTP concentration to 28 μM (Fig. 11c). In the solvent control, the polymerase assay produced 6332 ± 140 pmol of product, which was taken as 100% activity for measuring the effect of ART. There was a 38% reduction in polymerase activity at 4.8 μM ART, a 26% reduction with 19.5 μM (EC_{50}) ART and 40% reduction in polymerase activity at maximum conc. of 78 μM (Fig. 11d). These results indicate that ART inhibits HEV replication by directly targeting the activities of two important HEV enzymes: RdRp and helicase.

Discussion

HEV is one of the leading causes of acute viral hepatitis in adults in India. HEV infection mostly follows a self-limited course; however, a small proportion of individuals show higher disease severity, especially patients suffering from other liver infections or liver diseases. Acute HEV-1 infections in pregnancy are associated with high mortality rates of ~25%. HEV-3 infections are exclusively found in developed countries and show zoonotic transmission [11, 18]. Chronic HEV-3 infections have been reported in immunosuppressed individuals and found to be associated with extrahepatic manifestations such as neurological and kidney complications [62–64]. RBV and PEG-IFNα have been used in the treatment of both acute and chronic hepatitis E

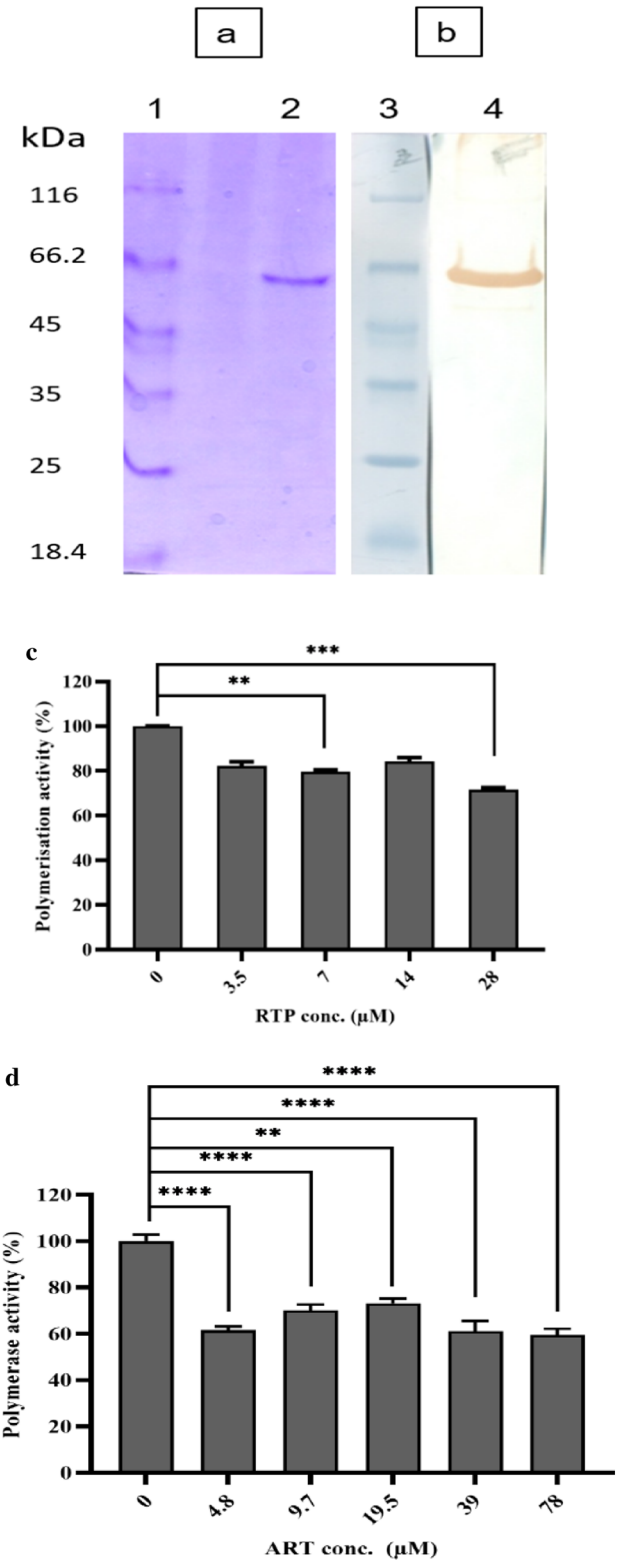

Fig. 11 Determination of the polymerase activity of the HEV-1 RdRp protein in the presence of drugs. HEV-1 RdRp was purified first using an Ni-NTA chromatography column, followed by gel-filtration chromatography, and fractions containing protein of the expected size were pooled. (a) Purified RdRp protein (56 kDa) was analysed by 10% SDS-PAGE with Coomassie brilliant blue staining. Lane 1, protein molecular weight marker (Fermentas SM0431); lane 2, HPLC-purified RdRp protein. (b) The HEV-1 replicase protein was transferred on to nitrocellulose membrane and detected using an anti-His antibody. Lane 3, protein molecular weight marker; lane 4, HPLC-purified protein. Polymerase activity was evaluated in the presence of different concentrations of (c) RTP and (d) ART. The enzymatic activity of the protein without drug treatment was considered 100%, and the percent inhibition of activity at different RTP and ART concentrations was calculated. Three independent experiments were performed in triplicate for each concentration of the drug.

patients; however, due to severe side effects, these drugs have limited application. Long-term use of ribavirin leads to side effects such as hemolytic anemia, pruritus, fatigue, and upper respiratory symptoms [65]. Both RBV and PEG-IFNα are contraindicated in pregnant women, while PEG-IFNα cannot be used in organ transplant patients [10, 11]. Chronic hepatitis E patients need at least a 12-week RBV treatment to achieve a sustained virological response [29]. There are few reports on viral relapse associated with RBV treatment. *In vitro* studies have also shown that resistance mutations in the HEV polymerase can arise with RBV treatment [31, 32, 34]. Hence, the availability of drugs with potency and efficacy similar to or better than currently available options would be extremely useful for treating high-risk hepatitis E patients.

In the present study, we tested the antimalarial drugs CQ, HCQ, and ART against HEV. We carried out primary screening of drugs using an HEV-1 subgenomic replicon, which allows quantitative estimation of HEV replication by measurement of Rluc activity. However, use of this replicon permits the evaluation of the effect of drugs on HEV transcription, translation, and replication, but not on virus entry, encapsidation, and egress due to the lack of synthesis of ORF2 and ORF3 proteins and formation of virus particles. These drugs were tested at the MNTD to test whether they are potential inhibitors of HEV. At the highest possible dose, CQ showed 23% inhibition, HCQ showed 9% inhibition, and ART showed 59% inhibition, which was comparable to RBV (62%). ART was better tolerated by human hepatoma cells (CC_{50}, 189 ± 14.11 μM) than RBV (CC_{50}, 39 ± 5.9 μM). Both RBV and ART showed an increase in HEV inhibition in a dose-dependent manner, with EC_{50} values of 2.9 ± 0.53 μM and 19.51 ± 4.03 μM, respectively (Fig. 3a and b). Thus, RBV was found to be a more potent inhibitor, with a lower EC_{50} value than that of ART. Since the inhibitory activity of ART was evaluated using an HEV subgenomic replicon that lacks functional ORF2 and ORF3 proteins, it was tested further using a full genomic replicon. The active replication of the pSK HEV-2 FG infectious cDNA clone was confirmed by detection of the ORF2 protein using IFA (Fig. 4a). RBV and ART reduced ORF2 expression significantly after 72 h and 96 h, as determined by IFA and western blot analysis (Fig. 4b, c, and d). In agreement with the results obtained

Table 3 Inhibition of HEV-1 helicase and RdRp assessed using *in vitro* enzymatic assays

Drug	EC_{50} concentration (μM)	Helicase ATPase activity inhibition (%)	RdRp polymerase activity inhibition (%)
RTP	7 ± 0.2	16 ± 1.6	20 ± 0.73
ART	19.5 ± 4.03	24 ± 2.6	26 ± 1.9

EC_{50}, half-maximal effective concentration

with the subgenomic replicon, the full-genome replicon culture system also showed an 81% reduction in the number of cell-associated HEV RNA copies and a 69% reduction in cell-free RNA copies (representing virus particles released into the culture supernatant) with ART (Fig. 5a and b), confirming its anti-HEV activity. It is especially important to note that ART was also found to be effective against HEV-3 (43% inhibition), as this genotype is responsible for the majority of chronic HEV infections. It would be worthwhile to test the inhibitory effect of ART on HEV-4, HEV-5, HEV-7, and HEV-8 as well as recently reported rat HEV isolates that have been shown to cause sporadic human infections [25, 66, 67].

Since ART showed a similar effect in subgenomic and full genomic replicon culture systems, we hypothesized that ART possibly influences the activities of viral enzymes encoded by ORF1. We selected the RdRp and helicase enzymes for analysis, as these are crucial for viral transcription and genome replication. It was documented previously that anti-malarial drugs such as amodiaquine, lumefantrine, and pyrimethamine have potential antiviral activity against HEV-3. As docking of artemisinin, an analog of ART, with different HEV proteins showed low scores with HEV protease and RdRp, it was not investigated further [38]. Since our experiments showed effective inhibition of HEV-1 with ART, comparable to that observed with ribavirin, we performed a docking simulation with HEV helicase. At a stabilized docking pose, ART showed a binding energy of -7.4 kcal/mol (Fig. 8c and d), with hydrogen bond interactions with three Walker A motif residues (Gly 979, Lys 982, and Ser 983) and van der Waals interactions with Arg 984 in the active site of helicase. The predicted energy of binding of helicase to ATP (substrate) was -8.9 kcal/mol (Fig. 8a and b). HEV helicase belongs to the SF-1 family and has seven signature motifs (I, Ia, II, III, IV, V, and VI). The function of HEV helicase is to unwind RNA duplexes using ATP as an energy source. Our previous study showed that replacement of K (Lys) residues in the conserved Walker A motif XGXAGXGKT reduces the ATPase activity of the enzyme by ~70% [58]. This Lys residue binds to the beta and gamma phosphates of ATP-Mg^{2+} complexes. Notably, the docking results showed the interaction of ART with the Lys of the Walker A motif, indicating the possibility of an influence on the ATP hydrolysis function of HEV helicase. In addition, comparable binding scores of helicase to ATP (substrate) and ART (inhibitor) suggested that ATP and ART may compete for the NTP binding site of the helicase.

To confirm the *in silico* results, ATPase assays were carried out. ATPase assays performed in the presence of ART showed that enzymatic activity could be inhibited from 23% up to 55% with increasing concentrations of ART (Table 3). HEV helicase showed an increase in enzymatic activity with an increase in substrate concentration (ATP) and reached the 100% level in the presence of 100 μM ATP. However, pre-incubation of the enzyme with ART did not allow the enzymatic activity to reach to its 100% level, even with higher ATP concentrations. The maximum ATPase activity that could be achieved after pre-treatment with ART was 80%. However, with prior addition of ATP, the activity could be restored to 100% with an increase in ATP concentration from 100 μM to 200 μM (Fig 10a and b). These observations clearly indicate that there is direct competition between ART and ATP for ATP binding sites on helicase proteins. With higher binding affinity, ATP competed well with ART, and prior incubation of the enzyme with ATP probably blocked the binding site of the enzyme or prevented efficient binding of ART. While pre-incubation of the enzyme with ART in the absence of ATP resulted in an enzyme-ART complex, ATP, which has stronger binding affinity, rescued most, but not all, of the enzyme molecules by competing with ART.

Several successful studies have already been performed targeting the hepatitis C virus (HCV) helicase [68–71]. Despite drug repurposing being very popular, limited data are available for helicase inhibitors of HEV. Parvez *et al.* have confirmed the critical role of helicase protein in HEV replication by saturation mutation analysis, which was further confirmed by replicon-based *in vitro* experiments [72]. A study on SARS-CoV-2 helicase 3D structure prediction and drug docking has shown that remdesivir has the highest binding affinity to the NTPase site of the helicase enzyme and was found to be the most effective helicase inhibitor among the potential drug molecules screened [73]. In another study, ivermectin, an FDA-approved antiparasitic drug, was predicted to be a SARS-CoV-2 helicase inhibitor using an *in silico* approach [74]. Elbasvir, an FDA-approved drug used for the treatment of chronic hepatitis C, was predicted to be an effective helicase inhibitor when docked against the SARS-CoV-2 helicase structure [75]. The SARS-CoV-2 nonstructural protein 13 (nsp13) exhibits NTPase and RNA helicase activities that can hydrolyze all types of NTPs and unwind RNA helices in an ATP-dependent manner. Both coronaviruses and HEV belong to the alphavirus-like superfamily of viruses. Since the activity of SARS-CoV-2 helicase is analogous to that of HEV RNA helicase [76], drugs

that are found to be potent SARS-CoV helicase inhibitors could also have potential as HEV helicase inhibitors.

The observation that ART showed competitive binding at the NTP binding site of HEV helicase compelled us also to test the effect of ART on HEV RdRp activity. We used ribavirin triphosphate (RTP) for comparison instead of ribavirin in the *in vitro* HEV polymerase assays. RTP and ART treatment resulted in 20% and 26% reduction in polymerase activity at their respective EC_{50} concentrations (Table 3). However, ART treatment resulted in a 38% reduction at a lower concentration of 4.8 μM. Thus, as anticipated, ART also inhibited the polymerase activity of HEV RdRp, possibly by competing for the NTP binding site of the enzyme. This could not be confirmed, because the 3D structure of HEV RdRp has not yet been determined.

Although ART treatment resulted in a reduction in the polymerase activity of HEV RdRp in an enzymatic assay, its exact site of action is not clear. Examples of HEV polymerase inhibitors include direct-acting antivirals (DAAs), which were originally used against hepatitis C virus but were found to be effective against HEV as well. Daclatasvir is a second-generation DAA that acts as a NS5A polymerase inhibitor, whereas sofosbuvir is a third-generation DAA that acts as a nucleosidic NS5B polymerase inhibitor against HCV. Daclatasvir and sofosbuvir have been used in combination with ribavirin for HEV treatment [77–79]. Other potential replicase inhibitors with reported activity against HEV include 2'-C-methylcytidine [80], mycophenolic acid [81], NITD008 [82], and zinc [55], but none of these studies have been taken further.

Our study is the first to show that ART hinders HEV replication by targeting two nonstructural proteins (helicase and RdRp). ART is a water-soluble semisynthetic derivative of the sesquiterpene lactone artemisinin with a short half-life and a moderate therapeutic index that is well tolerated by adults, children, and pregnant women [83–87]. It is formulated for intravenous, rectal, and oral administration [88]. ART has preferable pharmacokinetic properties and better effectiveness when compared to its parent artemisinin compound. ART has been found to be safe, stable, and well tolerated, but it occasionally may cause mild to moderate headache, nausea, vomiting, fatigue, anorexia, or severe hemolytic anaemia as side effects [89]. It was observed that ART is well tolerated when administered orally, and T_{max} is achieved in less than one hour, whereas the drug is eliminated from the body with a half-life of 21-72 minutes. In clinical trials, 600-1200 mg of ART was administered orally per day for a period of 5 days as a monotherapy or 200-800 mg per day orally for a period of 3 days in combination therapy for malaria treatment [90]. *In silico* toxicity studies revealed no risk of reproductive or developmental toxicity due to ART, but it may be moderately mutagenic, tumorigenic, and hepatotoxic if used in high doses for a long time [91].

Ribavirin is the current drug of choice for hepatitis E. In this study, the therapeutic indices of RBV and ART were 6.38 and 9.68, respectively, indicating that ART could be a better-tolerated drug than RBV (Table 1). ART monotherapy is the first line of drug treatment for severe malaria. ART is recommended by WHO for the treatment of malaria in pregnant women, especially during the second and third trimesters. Considering this and its low toxicity profile, ART can potentially be used for the treatment of hepatitis E.

In conclusion, ART inhibits the replication of both HEV-1 and HEV-3. It acts as a direct-acting antiviral and inhibits the activities of the HEV polymerase and helicase. Its wide-ranging antiviral activity, satisfactory bioavailability, and comparatively few adverse events make ART an attractive candidate for antiviral therapy against HEV. Hence, it can be a safe option for the treatment of HEV infection in high-risk individuals, including pregnant women, and deserves further evaluation in animal models.

Supplementary Information The online version contains supplementary material available at https://doi.org/10.1007/s00705-023-05770-1.

Acknowledgments The plasmids pSK-HEV-2 and pSK P6-Rluc were provided by Dr. S. Emerson, National Institutes of Health, Bethesda, MD, USA, and pSK-HEV-Rluc was provided by Dr. X. J. Meng, Virginia Tech, Blacksburg, VA, USA.

Author contributions All authors contributed to the study's conception and design under the guidance of KL and SC. Drug testing experiments were executed by NB and NT. AP performed the immunofluorescence assays, and statistical data analysis was performed by NB. Bioinformatics data were analyzed by MA. The first draft of the manuscript was written by NB and MA, and all authors commented on previous versions of the manuscript. All authors read and approved the final manuscript.

Funding This work was supported by the Indian Council of Medical Research (grant number: ISRM/12(06)/2019 ID 2018-2807). Author Neha Bhise received financial support from Union Grant Commission during her period of research.

Data availability All data generated or analyzed during this study are included in this published article and its supplementary PDF file.

Declarations

Conflict of interest The authors have no relevant financial or non-financial interests to disclose.

References

1. WHO Factsheet Hepatitis E [Internet]. https://www.who.int/news-room/fact-sheets/detail/hepatitis-e
2. Abbas Z, Afzal R (2014) Hepatitis E: when to treat and how to treat. Antivir Ther 19(2):125–131. https://doi.org/10.3851/IMP2705

3. Lapa D, Capobianchi MR, Garbuglia AR (2015) Epidemiology of hepatitis E virus in European countries. Int J Mol Sci 16(10):25711–25743. https://doi.org/10.3390/ijms161025711
4. Passos-Castilho AM, de Sena A, Geraldo A, Spada C, Granato CF (2016) High prevalence of hepatitis E virus antibodies among blood donors in Southern Brazil. J Med Virol 88(2):361–364. https://doi.org/10.1002/jmv.24336
5. Arankalle VA (2012) Hepatitis e in India. Proc Natl Acad Sci Sect B Biol Sci 82(1):43–53. https://doi.org/10.1007/s40011-011-0004-y
6. Chauhan NT, Prajapati P, Trivedi AV, Bhagyalaxmi A (2010) Epidemic investigation of the jaundice outbreak in Girdharnagar, Ahmedabad, Gujarat, India, 2008. Indian J Commun Med 35(2):294–297. https://doi.org/10.4103/0970-0218.66864
7. El-Mokhtar MA, Karam-Allah Ramadan H, Abdel Hameed MR, Kamel AM, Mandour SA, Ali M, Abdel-Malek MAY, Abd El-Kareem DM, Adel S, Salama EH, Khalaf KAB, Sayed IM (2021) Evaluation of hepatitis E antigen kinetics and its diagnostic utility for prediction of the outcomes of hepatitis E virus genotype 1 infection. Virulence 12(1):1334–1344. https://doi.org/10.1080/21505594.2021.1922027
8. Sayed IM, El-Mokhtar MA, Mahmoud MAR, Elkhawaga AA, Gaber S, Seddek NH, Abdel-Wahid L, Ashmawy AM, Alkareemy EAR (2021) Clinical outcomes and prevalence of hepatitis e virus (Hev) among non-a-c hepatitis patients in Egypt. Infect Drug Resist 14:59–69. https://doi.org/10.2147/IDR.S289766
9. Khuroo MS, Teli MR, Skidmore S, Sofi MA, Khuroo MI (1981) Incidence and severity of viral hepatitis in pregnancy. Am J Med 70(2):252–255. https://doi.org/10.1016/0002-9343[81]90758-0
10. Patra S, Kumar A, Shubha D, Trivedi S, Puri M, Sarin SK (2007) Maternal and fetal outcomes in pregnant women with acute hepatitis E virus infection. www.annals.org. https://doi.org/10.7326/0003-4819-147-1-200707030-00005
11. Dalton HR, Izopet J (2018) Transmission and epidemiology of hepatitis e virus genotype 3 and 4 infections. Cold Spring Harb Perspect Med 8(11):1–20. https://doi.org/10.1101/CSHPERSPECT.A032144
12. Hoofnagle JH, Nelson KE, Purcell RH (2012) Hepatitis E. N Engl J Med 367(13):1237–1244. https://doi.org/10.1056/nejmra1204512
13. Geng Y, Zhang H, Huang W, Harrison TJ, Geng K, Li Z, Wang Y (2014) Persistent hepatitis E virus genotype 4 infection in a child with acute lymphoblastic leukemia. Hepat Mon 14(1):e15618. https://doi.org/10.5812/hepatmon.15618
14. Lachish T, Erez O, Daudi N, Shouval D, Schwartz E (2015) Acute hepatitis E virus in pregnant women in Israel and in other industrialized countries. J Clin Virol 73:20–24. https://doi.org/10.1016/j.jcv.2015.10.011
15. Fraga M, Doerig C, Moulin H, Bihl F, Brunner F, Müllhaupt B, Ripellino P, Semela D, Stickel F, Terziroli Beretta-Piccoli B, Aubert V, Telenti A, Greub G, Sahli R, Moradpour D (2018) Hepatitis E virus as a cause of acute hepatitis acquired in Switzerland. Liver Int 38(4):619–626. https://doi.org/10.1111/liv.13557
16. Robins AEM, Bowden DJ, Gelson WTH (2018) Chronic genotype 1 hepatitis e infection from immunosuppression for ileo-colonic Crohn's disease. Oxf Med Case Reports 2018(9):278–281. https://doi.org/10.1093/omcr/omy059
17. Rathi S, Duseja A, Thakur V, Ratho RK, Singh MP, Taneja S, Das A, Aggarwal R, Dhiman RK, Chawla YK (2021) Chronic hepatitis E with genotype 1—masquerading as allograft rejection after liver transplantation. J Clin Exp Hepatol 11(3):400–403. https://doi.org/10.1016/j.jceh.2020.07.006
18. Kamar N, Selves J, Mansuy J-M, Ouezzani L, Péron J-M, Guitard J, Cointault O, Esposito L, Abravanel F, Danjoux M, Durand D, Vinel J-P, Izopet J, Rostaing L (2008) Hepatitis E virus and chronic hepatitis in organ-transplant recipients. N Engl J Med 358(8):811–817. https://doi.org/10.1056/nejmoa0706992
19. Purcell RH, Emerson SU (2008) Hepatitis E: an emerging awareness of an old disease. J Hepatol 48(3):494–503. https://doi.org/10.1016/j.jhep.2007.12.008
20. Panda SK, Thakral D, Rehman S (2007) Hepatitis E virus. Rev Med Virol 17(3):151–180. https://doi.org/10.1002/rmv.522
21. Tam AW, Smith MM, Guerra ME, Huang CC, Bradley DW, Fry KE, Reyes GR (1991) Hepatitis E virus [HEV]: molecular cloning and sequencing of the full-length viral genome. Virology 185(1):120–131. https://doi.org/10.1016/0042-6822[91]90760-9
22. Murrison LB, Sherman KE (2017) The enigma of hepatitis E virus. Gastroenterology and Hepatology 13(8):484–491 (**PMID: 28867980**)
23. Gouttenoire J, Pollán A, Abrami L, Oechslin N, Mauron J, Matter M, Oppliger J, Szkolnicka D, Dao Thi VL, van der Goot FG, Moradpour D (2018) Palmitoylation mediates membrane association of hepatitis E virus ORF3 protein and is required for infectious particle secretion. PLoS Pathog 14(12):1–24. https://doi.org/10.1371/journal.ppat.1007471
24. Nair VP, Anang S, Subramani C, Madhvi A, Bakshi K, Srivastava A, Shalimar, Nayak B, Ranjith Kumar CT, Surjit M (2016) Endoplasmic reticulum stress induced synthesis of a novel viral factor mediates efficient replication of genotype-1 hepatitis E virus. PLoS Pathog 12(4):1–31. https://doi.org/10.1371/journal.ppat.1005521
25. Ferri G, Vergara A (2021) Hepatitis E virus in the food of animal origin: a review. Foodborne Pathog Dis 18(6):368–377. https://doi.org/10.1089/fpd.2020.2896
26. Yugo DM, Meng XJ (2013) Hepatitis E virus: foodborne, waterborne and zoonotic transmission. Int J Environ Res Public Health 10(10):4507–4533. https://doi.org/10.3390/ijerph10104507
27. Khuroo MS, Khuroo MS, Khuroo NS (2016) Transmission of hepatitis E virus in developing countries. Viruses 8(9):253. https://doi.org/10.3390/v8090253
28. Sayed IM, Abdelwahab SF (2022) Is hepatitis E virus a neglected or emerging pathogen in Egypt? Pathogens 11(11):1337. https://doi.org/10.3390/pathogens11111337
29. Kamar N, Abravanel F, Selves J, Garrouste C, Esposito L, Lavayssière L, Cointault O, Ribes D, Cardeau I, Nogier MB, Mansuy JM, Muscari F, Peron JM, Izopet J, Rostaing L (2010) Influence of immunosuppressive therapy on the natural history of genotype 3 hepatitis-E virus infection after organ transplantation. Transplantation 89(3):353–360. https://doi.org/10.1097/TP.0b013e3181c4096c
30. Kamar N, Garrouste C, Haagsma EB, Garrigue V, Pischke S, Chauvet C, Dumortier J, Cannesson A, Cassutoviguier E, Thervet E, Conti F, Lebray P, Dalton HR, Santella R, Kanaan N, Essig M, Mousson C, Radenne S, Roqueafonso AM, Rostaing L (2011) Factors associated with chronic hepatitis in patients with hepatitis e virus infection who have received solid organ transplants. Gastroenterology 140(5):1481–1489. https://doi.org/10.1053/j.gastro.2011.02.050
31. Debing Y, Gisa A, Dallmeier K, Pischke S, Bremer B, Manns M, Wedemeyer H, Suneetha PV, Neyts J (2014) A mutation in the hepatitis e virus RNA polymerase promotes its replication and associates with ribavirin treatment failure in organ transplant recipients. Gastroenterology 147(5):1008-1011.e7. https://doi.org/10.1053/j.gastro.2014.08.040
32. Lhomme S, Kamar N, Nicot F, Ducos J, Bismuth M, Garrigue V, Petitjean-Lecherbonnier J, Ollivier I, Alessandri-Gradt E, Goria O, Barth H, Perrin P, Saune K, Dubois M, Carcenac R, Lefebvre C, Jeanne N, Abravanel F, Izopet J (2016) Mutation in the hepatitis E virus polymerase and outcome of ribavirin therapy. Antimicrob Agents Chemother 60(3):1608–1614. https://doi.org/10.1128/AAC.02496-15

33. Sayed IM, Vercouter AS, Abdelwahab SF, Vercauteren K, Meuleman P (2015) Is hepatitis E virus an emerging problem in industrialized countries? Hepatology 62(6):1883–1892. https://doi.org/10.1002/hep.27990
34. Todt D, Gisa A, Radonic A, Nitsche A, Behrendt P, Suneetha PV, Pischke S, Bremer B, Brown RJP, Manns MP, Cornberg M, Thomas Bock C, Steinmann E, Wedemeyer H (2016) In vivo evidence for ribavirin-induced mutagenesis of the hepatitis E virus genome. Gut 65(10):1733–1743. https://doi.org/10.1136/gutjnl-2015-311000
35. Wu C, Wu X, Xia J (2020) Hepatitis e virus infection during pregnancy. Virol J 17(1):1–11. https://doi.org/10.1186/s12985-020-01343-9
36. Dao Thi VL, Debing Y, Wu X, Rice CM, Neyts J, Moradpour D, Gouttenoire J (2016) Sofosbuvir inhibits hepatitis E virus replication in vitro and results in an additive effect when combined with ribavirin. Gastroenterology 150(1):82-85.e4. https://doi.org/10.1053/j.gastro.2015.09.011
37. Rudrapal M, Khairnar SJ, Jadhav AG (2020) Drug repurposing (DR): an emerging approach in drug discovery. Drug Repurposing Hypothesis Mol Aspects Ther Appl. https://doi.org/10.5772/intechopen.93193
38. Tietcheu Galani BR, Ayissi Owona VB, Guemmogne Temdie RJ, Metzger K, Atsama Amougou M, Djamen Chuisseu PD, Fondjo Kouam A, Ngounoue Djuidje M, Aliouat-Denis C-M, Cocquerel L, Fewou Moundipa P (2021) In silico and in vitro screening of licensed antimalarial drugs for repurposing as inhibitors of hepatitis E virus. In Silico Pharmacol 9(1):1–17. https://doi.org/10.1007/s40203-021-00093-y
39. Tu Y (1999) The development of new antimalarial drugs: qinghaosu and dihydro-qinghaosu. Chin Med J [Engl] 112(11):976–977 (**PMID: 11721477**)
40. Nosten F, McGready R, d'Alessandro U, Bonell A, Verhoeff F, Menendez C, Mutabingwa T, Brabin B (2008) Antimalarial drugs in pregnancy: a review. Curr Drug Saf 1(1):1–15. https://doi.org/10.2174/157488606775252584
41. Kouakou YI, Tod M, Leboucher G, Lavoignat A, Bonnot G, Bienvenu AL, Picot S (2019) Systematic review of artesunate pharmacokinetics: Implication for treatment of resistant malaria. Int J Infect Dis 89:30–44. https://doi.org/10.1016/j.ijid.2019.08.030
42. Efferth T, Sauerbrey A, Olbrich A, Gebhart E, Rauch P, Weber HO, Hengstler JG, Halatsch ME, Volm M, Tew KD, Ross DD, Funk JO (2003) Molecular modes of action of artesunate in tumor cell lines. Mol Pharmacol 64(2):382–394. https://doi.org/10.1124/mol.64.2.382
43. Utzinger J, Xiao SH, Tanner M, Keiser J (2007) Artemisinins for schistosomiasis and beyond. Curr Opin Investig Drugs 8(2):105–116. https://doi.org/10.3851/imp1467
44. Siakallis G, Spandidos DA, Sourvinos G (2009) Herpesviridae and novel inhibitors. Antivir Ther 14(8):1051–1064. https://doi.org/10.3851/IMP1467
45. Chemaly RF, Hill JA, Voigt S, Peggs KS (2019) In vitro comparison of currently available and investigational antiviral agents against pathogenic human double-stranded DNA viruses: a systematic literature review. Antiviral Res 163(October 2018):50–58. https://doi.org/10.1016/j.antiviral.2019.01.008
46. Efferth T, Marschall M, Wang X, Huong SM, Hauber I, Olbrich A, Kronschnabl M, Stamminger T, Huang ES (2002) Antiviral activity of artesunate towards wild-type, recombinant, and ganciclovir-resistant human cytomegaloviruses. J Mol Med 80(4):233–242. https://doi.org/10.1007/s00109-001-0300-8
47. Zamidei L, Durval A, Bettocchi D, Luzzio MG, Bartoloni A, Consales G (2010) Efficacy and safety of quinine-artesunate in an HIV-positive patient with severe falciparum malaria. Minerva Anestesiol 76(1):66–69 (**Epub 2009 Oct 7. PMID: 20125075**)
48. Wohlfarth C, Efferth T (2009) Natural products as promising drug candidates for the treatment of hepatitis B and C. Acta Pharmacol Sin 30(1):25–30. https://doi.org/10.1038/aps.2008.5
49. Romero MR, Efferth T, Serrano MA, Castaño B, MacIas RIR, Briz O, Marin JJG (2005) Effect of artemisinin/artesunate as inhibitors of hepatitis B virus production in an "in vitro" replicative system. Antiviral Res 68(2):75–83. https://doi.org/10.1016/j.antiviral.2005.07.005
50. Dai R, Xiao X, Peng F, Li M, Gong G (2016) Artesunate, an antimalarial drug, has a potential to inhibit HCV replication. Virus Genes. https://doi.org/10.1007/s11262-015-1285-7
51. Emerson SU, Zhang M, Meng XJ, Nguyen H, St Claire M, Govindarajan S, Huang YK, Purcell RH (2001) Recombinant hepatitis E virus genomes infectious for primates: Importance of capping and discovery of a cis-reactive element. Proc Natl Acad Sci USA 98(26):15270–15275. https://doi.org/10.1073/pnas.251555098
52. Shukla P, Nguyen HT, Faulk K, Mather K, Torian U, Engle RE, Emerson SU (2012) Adaptation of a genotype 3 hepatitis E virus to efficient growth in cell culture depends on an inserted human gene segment acquired by recombination. J Virol 86(10):5697–5707. https://doi.org/10.1128/jvi.00146-12
53. Cao D, Huang Y-W, Meng X-J (2010) The nucleotides on the stem-loop RNA structure in the junction region of the hepatitis E virus genome are critical for virus replication. J Virol 84(24):13040–13044. https://doi.org/10.1128/jvi.01475-10
54. Sun D, Nassal M (2006) Stable HepG2- and Huh7-based human hepatoma cell lines for efficient regulated expression of infectious hepatitis B virus. J Hepatol 45(5):636–645. https://doi.org/10.1016/j.jhep.2006.05.019
55. Kaushik N, Subramani C, Anang S, Muthumohan R, Shalimar, Nayak B, Ranjith-Kumar CT, Surjit M (2017) Zinc salts block hepatitis E virus replication by inhibiting the activity of viral RNA-dependent RNA polymerase. J Virol 91(21):e00754-e817. https://doi.org/10.1128/jvi.00754-17
56. Devhare PB, Desai S, Lole KS (2016) Innate immune responses in human hepatocyte-derived cell lines alter genotype 1 hepatitis E virus replication efficiencies OPEN. Nat Publ Group. https://doi.org/10.1038/srep26827
57. Karpe YA, Lole KS (2010) NTPase and 5' to 3' RNA duplex-unwinding activities of the hepatitis E virus helicase domain. J Virol 84(7):3595–3602. https://doi.org/10.1128/JVI.02130-09
58. Mhaindarkar V, Sharma K, Lole KS (2014) Mutagenesis of hepatitis E virus helicase motifs: effects on enzyme activity. Virus Res 179(1):26–33. https://doi.org/10.1016/j.virusres.2013.11.022
59. Mahilkar S, Paingankar MS, Lole KS (2016) Hepatitis E virus RNA-dependent RNA polymerase: RNA template specificities, recruitment and synthesis. J Gen Virol 97(9):2231–2242. https://doi.org/10.1099/jgv.0.000528
60. Debing Y, Moradpour D, Neyts J, Gouttenoire J (2016) Update on hepatitis e virology: implications for clinical practice. J Hepatol 65(1):200–212. https://doi.org/10.1016/j.jhep.2016.02.045
61. Kinast V, Burkard TL, Todt D, Steinmann E (2019) Hepatitis E virus drug development. Viruses 11(6):1–16. https://doi.org/10.3390/v11060485
62. Dalton HR, Bendall RP, Keane FE, Tedder RS, Ijaz S (2009) Persistent carriage of hepatitis E virus in patients with HIV infection. N Engl J Med 361(10):1025–1027. https://doi.org/10.1056/nejmc0903778
63. Kamar N, Abravanel F, Garrouste C, Cardeau-Desangles I, Mansuy JM, Weclawiak H, Izopet J, Rostaing L (2010) Three-month pegylated interferon-alpha-2a therapy for chronic hepatitis E virus infection in a haemodialysis patient. Nephrol Dial Transplant 25(8):2792–2795. https://doi.org/10.1093/ndt/gfq282
64. Pischke S, Hartl J, Pas SD, Lohse AW, Jacobs BC, Van der Eijk AA (2017) Hepatitis E virus: infection beyond the liver? J Hepatol 66(5):1082–1095. https://doi.org/10.1016/j.jhep.2016.11.016

65. Di Bisceglie AM, Conjeevaram HS, Fried MW, Sallie R, Park Y, Yurdaydin C, Swain M, Kleiner DE, Mahaney K, Hoofnagle JH (1995) Ribavirin as therapy for chronic hepatitis C. A randomized, double-blind, placebo-controlled trial. Ann Intern Med 123(12):897–903. https://doi.org/10.7326/0003-4819-123-12-199512150-00001
66. Sridhar S, Yip CCY, Wu S, Cai J, Zhang JX, Leung KH, Chung TWH, Chan FW, Chan WM, Teng JLL et al (2018) Rat hepatitis E virus as cause of persistent hepatitis after liver transplant. Emerg Infect Dis 24:2241–2250. https://doi.org/10.3201/eid2412.180937
67. Andonov A, Robbins M, Borlang J, Cao J, Hatchette T, Stueck A, Deschambault Y, Murnaghan K, Varga J, Johnston L (2019) Rat hepatitis E virus linked to severe acute hepatitis in an immunocompetent patient. J Infect Dis 220:951–955. https://doi.org/10.1093/infdis/jiz025
68. Mukherjee S, Weiner WS, Schroeder CE, Simpson DS, Hanson AM, Sweeney NL, Marvin RK, Ndjomou J, Kolli R, Isailovic D, Schoenen FJ, Frick DN (2014) Ebselen inhibits hepatitis C virus NS3 helicase binding to nucleic acid and prevents viral replication. ACS Chem Biol 9(10):2393–2403. https://doi.org/10.1021/cb500512z
69. Irshad M, Gupta P, Irshad K (2018) Molecular targeting of antiviral drugs used against hepatitis C virus infection. Hepatoma Res 4(6):23. https://doi.org/10.20517/2394-5079.2018.25
70. Anang S, Kaushik N, Surjit M (2018) Recent advances towards the development of a potent antiviral against the hepatitis E virus. J Clin Transl Hepatol 6(3):310–316. https://doi.org/10.14218/JCTH.2018.00005
71. Jin G, Lee J, Lee K (2017) Chemical genetics-based development of small molecules targeting hepatitis C virus. Arch Pharmacal Res 40(9):1021–1036. https://doi.org/10.1007/s12272-017-0949-3
72. Parvez MK, Subbarao N (2018) Molecular analysis and modeling of hepatitis E virus helicase and identification of novel inhibitors by virtual screening. Biomed Res Int. https://doi.org/10.1155/2018/5753804
73. Satpathy R (2020) In Silico modeling and docking study of potential helicase (nonstructural proteins) inhibitors of novel coronavirus 2019 (severe acute respiratory syndrome coronavirus 2). Biomed Biotechnol Res J 4(4):330–336. https://doi.org/10.4103/bbrj.bbrj_149_20
74. Khater S, Das G (2020). Repurposing Ivermectin to inhibit the activity of SARS CoV2 helicase: possible implications for COVID 19 therapeutics. https://doi.org/10.31219/osf.io/8dseq
75. Balasubramaniam M, Reis RJS (2020) Computational target-based drug repurposing of elbasvir, an antiviral drug predicted to bind multiple SARS-CoV-2 proteins. ChemRxiv The Preprint Server for Chemistry. https://doi.org/10.26434/chemrxiv.12084822
76. Shu T, Huang M, Wu D, Ren Y, Zhang X, Han Y, Mu J, Wang R, Qiu Y, Zhang DY, Zhou X (2020) SARS-coronavirus-2 Nsp13 possesses NTPase and RNA helicase activities that can be inhibited by bismuth salts. Virologica Sinica 35(3):321–329. https://doi.org/10.1007/s12250-020-00242-1
77. Gamal N, Gitto S, Andreone P (2016) Efficacy and safety of daclatasvir in hepatitis C: an overview. J Clin Transl Hepatol 4(4):336–344. https://doi.org/10.14218/JCTH.2016.00038
78. Donnelly MC, Imlach SN, Abravanel F, Ramalingam S, Johannessen I, Petrik J, Fraser AR, Campbell JD, Bramley P, Dalton HR, Hayes PC, Kamar N, Simpson KJ (2017) Sofosbuvir and daclatasvir anti-viral therapy fails to clear HEV viremia and restore reactive T cells in a HEV/HCV co-infected liver transplant recipient. Gastroenterology 152(1):300–301. https://doi.org/10.1053/j.gastro.2016.05.060
79. Qu C, Xu L, Yin Y, Peppelenbosch MP, Pan Q, Wang W (2017) Nucleoside analogue 2'-C-methylcytidine inhibits hepatitis E virus replication but antagonizes ribavirin. Adv Virol 162(10):2989–2996. https://doi.org/10.1007/s00705-017-3444-8
80. Wang Y, Zhou X, Debing Y, Chen K, Van Der Laan LJW, Neyts J, Janssen HLA, Metselaar HJ, Peppelenbosch MP, Pan Q (2014) Calcineurin inhibitors stimulate and mycophenolic acid inhibits replication of hepatitis e virus. Gastroenterology 146(7):1775–1783. https://doi.org/10.1053/j.gastro.2014.02.036
81. Netzler NE, Tuipulotu DE, Vasudevan SG, Mackenzie JM, White PA (2019) Antiviral candidates for treating hepatitis E virus infection. Antimicrob Agents Chemother. https://doi.org/10.1128/AAC.00003-19
82. Drug Central 2021: Online drug Compendium [https://drugcentral.org/drugcard/247]
83. Olliaro PL, Nair NK, Sathasivam K, Mansor SM, Navaratnam V (2001) Pharmacokinetics of artesunate after single oral administration to rats. BMC Pharmacol 1:1–4. https://doi.org/10.1186/1471-2210-1-12
84. Qidwai T, Yadav DK, Khan F, Dhawan S, Bhakuni RS (2012) QSAR, docking and ADMET studies of artemisinin derivatives for antimalarial activity targeting plasmepsin II, a hemoglobin-degrading enzyme from *P. falciparum*. Curr Pharm Des 18(37):6133–6154. https://doi.org/10.2174/138161212803582397
85. Onyamboko MA, Meshnick SR, Fleckenstein L, Koch MA, Atibu J, Lokomba V, Douoguih M, Hemingway-Foday J, Wesche D, Ryder RW, Bose C, Wright LL, Tshefu AK, Capparelli EV (2011) Pharmacokinetics and pharmacodynamics of artesunate and dihydroartemisinin following oral treatment in pregnant women with asymptomatic *Plasmodium falciparum* infections in Kinshasa DRC. Malar J 10(1):49. https://doi.org/10.1186/1475-2875-10-49
86. Morris CA, Duparc S, Borghini-Fuhrer I, Jung D, Shin CS, Fleckenstein L (2011) Review of the clinical pharmacokinetics of artesunate and its active metabolite dihydroartemisinin following intravenous, intramuscular, oral or rectal administration. Malar J 10:1–17. https://doi.org/10.1186/1475-2875-10-263
87. Barradell LB, Fitton A (1995) Artesunate: a review of its pharmacology and therapeutic efficacy in the treatment of malaria. Drugs 50(4):714–741. https://doi.org/10.2165/00003495-199550040-00009
88. Batty KT, Thu LTA, Davis TME, Ilett KF, Mai TX, Hung NC, Tien NP, Powell SM, Thien HV, Binh TQ, Kim NV (1998) A pharmacokinetic and pharmacodynamic study of intravenous vs oral artesunate in uncomplicated falciparum malaria. Br J Clin Pharmacol 45(2):123–129. https://doi.org/10.1046/j.1365-2125.1998.00655.x
89. Newton P, Suputtamongkol Y, Teja-Isavadharm P, Pukrittayakamee S, Navaratnam V, Bates I, White N (2000) Antimalarial bioavailability and disposition of artesunate in acute falciparum, malaria. Antimicrob Agents Chemother 44(4):972–977. https://doi.org/10.1128/AAC.44.4.972-977.2000
90. Efferth T, Romero MR, Wolf DG, Stamminger T, Marin JJG, Marschall M (2008) The antiviral activities of artemisinin and artesunate. Clin Infect Dis 47(6):804–811. https://doi.org/10.1086/591195
91. Uckun FM, Saund S, Windlass H, Trieu V (2021) Repurposing anti-malaria phytomedicine artemisinin as a COVID-19 drug. Front Pharmacol 12(March):1–5. https://doi.org/10.3389/fphar.2021.649532